SUPPLEMENTARY INFORMATION

A NIR Fluorescent Rosol Dye Tailored toward Lymphatic Mapping Applications

Kenneth S. Hettie[1†], Jessica L. Klockow[1†], Timothy E. Glass[2], Frederick T. Chin[1*]

[1]Molecular Imaging Program at Stanford (MIPS), Department of Radiology, Stanford University School of Medicine, Stanford, California 94305
[2]Department of Chemistry, University of Missouri, Columbia, MO 65211
*Corresponding author
[†]Equal contribution

TABLE OF CONTENTS **PAGE**

1. Generic Molecular Fluorescent Dyes Commonly Used for Lymphatic Mapping Applications

Table S1. Chemical structures, photophysical and physical properties of the limited set of generic molecular fluorescent dyes commonly used for lymphatic fluorescence mapping applications.

	Fluorescein	**Methylene Blue (MB)**	**Indocyanine Green (ICG)**
	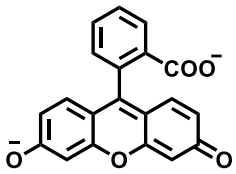	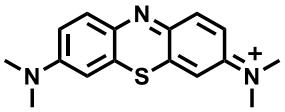	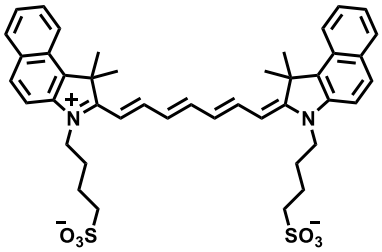
M.W. (g/mol)	330.30 (at pH 7.4 as drawn) 332.31 (neutral form) 376.27 (disodium salt)	284.40 (at pH 7.4 as drawn) 319.85 (chloride salt)	751.98 (at pH 7.4 as drawn) 774.96 (monosodium salt)
λ_{abs} (nm) in aqueous buffer	434 (neutral species) 450 & 470 (anionic species) 490 (dianionic species)	664	785
λ_{em} (nm) in aqueous buffer	520	690	822
Stokes shift (nm)	30	26	37
pK_a	2.1, 4.3, ~6.4	<2.0	3.3

2. Computational Methods & Correlation Plots

red arrow = torsion angle about the N-C3' bond

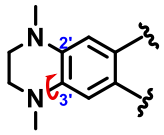

N-Methyl-THQ-Rosol

red arrow = torsion angle about the N-C2' bond

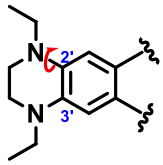

N-Ethyl-THQ-Rosol ("THQ-Rosol")

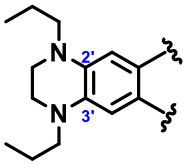

N-Propyl-THQ-Rosol

E_{LUMO} (hartrees)	-0.07337	-0.06856	-0.06821
E_{HOMO} (hartrees)	-0.18167	-0.17245	-0.17175
ΔE (hartrees)	0.10830	0.10389	0.10354
Torsion angle N-C2' (θ)	18.24°	12.21°	15.47°
Torsion angle N-C3' (θ)	13.38°	10.34°	15.80°

Figure S1. Torsion Angles. Molecular modeling alongside DFT calculations provided the energy of the highest and lowest occupied molecular orbital values (E_{HOMO} and E_{LUMO}, respectively), the molecular orbital energy gap (ΔE), and torsion angles (θ) of additionally-explored N-substituted **THQ-Rosol** dye analogues, all of which have a larger/comparable molecular orbital energy gap and/or torsion angle relative to **THQ-Rosol**.

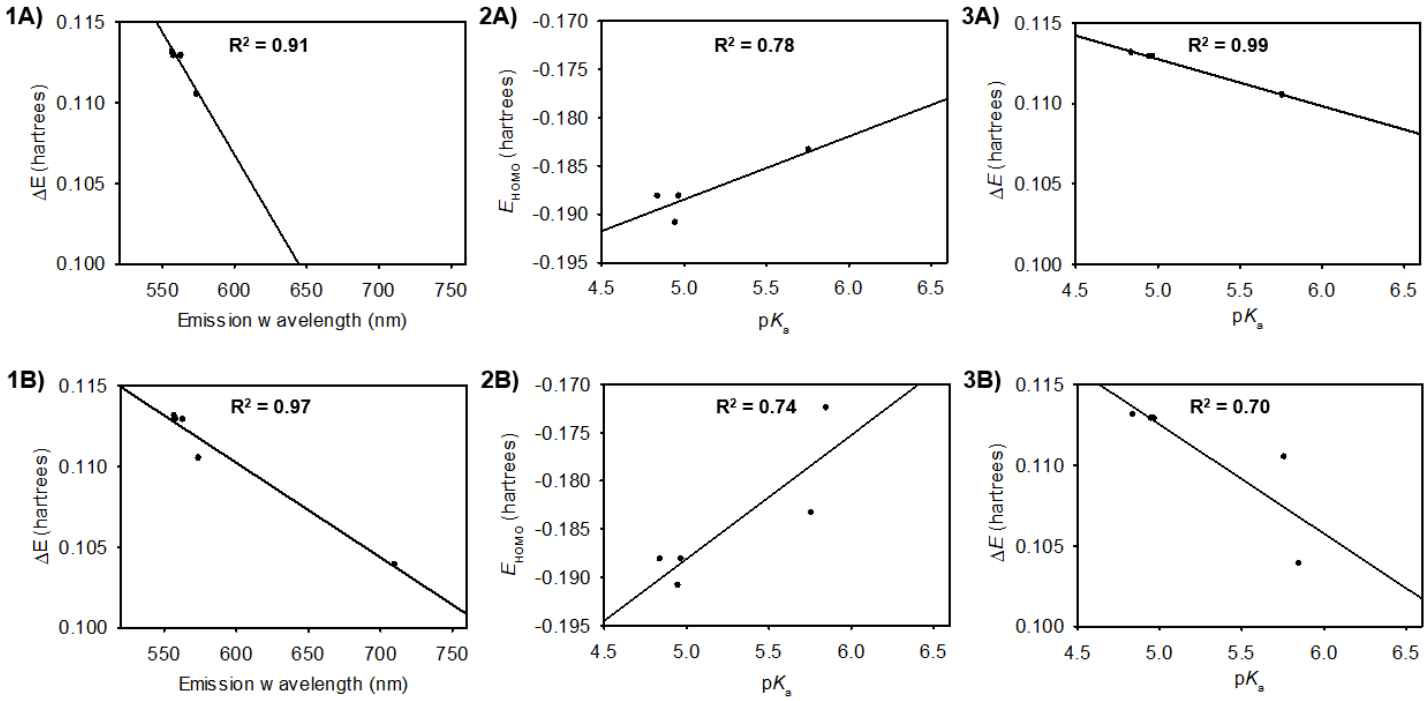

Figure S2. Linear Regression Analysis. Linear regression analyses of the calculated energetics in relation to the measured maximum fluorescence emission wavelength and experimentally-determined pK_a values. Plots in the top row (1A, 2A, 3A) correlate various calculated values/evaluated properties for the following fluorophores: **Me-Rosol**, **Et-Rosol**, **Pip-Rosol**, and **Jul-Rosol.** Plots in the bottom row (1B, 2B, 3B) include **THQ-Rosol** in the analysis and their accompanying coefficient of determination.

Table S2. Z-Matrices (Internal Coordinates) of Modeled Structures

Me-Rosol

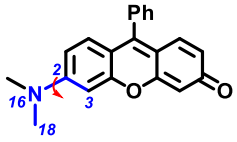

Et-Rosol

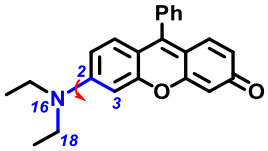

Pip-Rosol

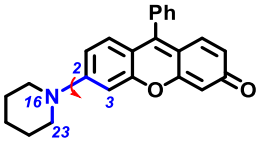

The Z-matrix for each modeled structure as provided by Gaussian, wherein each atom is labeled according to its numbering system.

Tag	Symbol	NA	NB	NC	Bond	Angle	Dihedral
1	C						
2	C	1			1.404		
3	C	2	1		1.404	115.49	
4	C	3	2	1	1.404	122.24	-1.28
5	C	4	3	2	1.388	121.46	0.53
6	C	5	4	3	1.397	117.38	0.29
7	O	4	3	2	1.370	116.19	-179.59
8	C	7	4	3	1.387	119.31	179.97
9	C	8	7	4	1.473	120.40	0.09
10	C	9	8	7	1.361	120.49	0.00
11	C	8	7	4	1.340	118.25	-179.90
12	C	11	8	7	1.476	121.13	179.97
13	C	12	11	8	1.478	117.66	0.07
14	C	13	12	11	1.340	120.67	-0.06
15	O	12	11	8	1.225	121.26	-179.91
16	N	2	1	6	1.400	122.30	179.12
17	C	16	2	1	1.462	119.19	13.35
18	C	16	2	1	1.463	118.77	163.72
19	C	10	9	8	1.485	120.41	179.99
20	C	19	10	9	1.401	120.22	-90.27
21	C	20	19	10	1.396	120.14	-179.83
22	C	21	20	19	1.395	120.03	0.12
23	C	22	21	20	1.395	120.11	0.09
24	C	23	22	21	1.396	120.03	-0.08
25	H	1	2	16	1.086	121.04	-0.81
26	H	3	2	1	1.085	120.93	178.33
27	H	6	5	4	1.088	121.03	179.46
28	H	11	8	7	1.082	122.26	-0.02
29	H	13	12	11	1.083	116.73	179.94
30	H	14	13	12	1.086	118.17	179.98
31	H	17	16	2	1.096	111.22	-179.01
32	H	17	16	2	1.095	111.25	-61.32
33	H	17	16	2	1.096	111.06	61.18
34	H	18	16	2	1.096	111.30	-178.09
35	H	18	16	2	1.096	111.08	-58.33
36	H	18	16	2	1.095	111.21	64.13
37	H	20	19	10	1.088	120.31	0.09
38	H	21	20	19	1.087	119.95	-179.98
39	H	22	21	20	1.087	119.94	179.95
40	H	23	22	21	1.087	120.01	179.82
41	H	24	23	22	1.088	119.55	179.81

Tag	Symbol	NA	NB	NC	Bond	Angle	Dihedral
1	C						
2	C	1			1.404		
3	C	2	1		1.404	115.26	
4	C	3	2	1	1.404	122.40	-0.03
5	C	4	3	2	1.388	121.45	-0.06
6	C	5	4	3	1.396	117.32	0.08
7	O	4	3	2	1.370	116.20	179.79
8	C	7	4	3	1.387	119.31	179.98
9	C	8	7	4	1.473	120.40	0.05
10	C	9	8	7	1.361	120.49	0.04
11	C	8	7	4	1.340	118.25	-179.95
12	C	11	8	7	1.476	121.13	179.98
13	C	12	11	8	1.478	117.66	0.00
14	C	13	12	11	1.340	120.67	0.01
15	O	12	11	8	1.225	121.26	-179.99
16	N	2	1	6	1.391	122.33	-179.91
17	C	16	2	1	1.470	122.12	-13.72
18	C	16	2	1	1.470	121.45	165.12
19	C	10	9	8	1.485	120.42	179.98
20	C	19	10	9	1.401	120.22	90.31
21	C	20	19	10	1.396	120.14	179.84
22	C	21	20	19	1.395	120.03	-0.13
23	C	22	21	20	1.395	120.11	-0.09
24	C	23	22	21	1.396	120.03	0.09
25	C	17	16	2	1.523	111.79	-72.65
26	C	18	16	2	1.521	111.45	94.20
27	H	1	2	16	1.086	120.94	-0.64
28	H	3	2	1	1.085	120.88	178.75
29	H	6	5	4	1.087	121.05	-179.89
30	H	11	8	7	1.082	122.26	-0.01
31	H	13	12	11	1.083	116.73	-179.99
32	H	14	13	12	1.086	118.17	-180.00
33	H	17	16	2	1.096	111.21	51.97
34	H	17	16	2	1.097	110.08	167.77
35	H	18	16	2	1.097	109.75	-145.37
36	H	18	16	2	1.096	111.72	-30.03
37	H	20	19	10	1.088	120.31	-0.09
38	H	21	20	19	1.087	119.95	179.97
39	H	22	21	20	1.087	119.94	-179.94
40	H	23	22	21	1.087	120.02	-179.81
41	H	24	23	22	1.088	119.56	-179.80
42	H	25	17	16	1.095	110.04	-177.41
43	H	25	17	16	1.094	111.24	-57.80
44	H	25	17	16	1.094	112.05	62.71
45	H	26	18	16	1.095	110.13	-177.33
46	H	26	18	16	1.094	111.82	-57.05
47	H	26	18	16	1.094	111.07	63.39

Tag	Symbol	NA	NB	NC	Bond	Angle	Dihedral
1	C						
2	C	1			1.405		
3	C	2	1		1.404	114.99	
4	C	3	2	1	1.405	122.47	2.57
5	C	4	3	2	1.387	121.52	-1.13
6	C	5	4	3	1.395	117.23	-0.55
7	O	4	3	2	1.370	116.16	178.94
8	C	7	4	3	1.387	119.31	-179.91
9	C	8	7	4	1.473	120.40	-0.13
10	C	9	8	7	1.360	120.48	0.02
11	C	8	7	4	1.340	118.26	179.87
12	C	11	8	7	1.476	121.13	-179.98
13	C	12	11	8	1.478	117.66	-0.07
14	C	13	12	11	1.340	120.67	0.06
15	O	12	11	8	1.225	121.26	179.90
16	N	2	1	6	1.402	122.02	-178.61
17	C	10	9	8	1.485	120.43	-180.00
18	C	17	10	9	1.401	120.22	-90.33
19	C	18	17	10	1.396	120.14	-179.84
20	C	19	18	17	1.395	120.03	0.13
21	C	20	19	18	1.395	120.11	0.08
22	C	21	20	19	1.396	120.03	-0.09
23	C	16	2	1	1.476	120.07	-172.19
24	C	23	16	2	1.530	110.05	82.86
25	C	24	23	16	1.531	111.00	55.76
26	C	25	24	23	1.531	111.78	-50.65
27	C	16	2	1	1.477	119.07	-29.68
28	H	1	2	16	1.085	121.29	-0.18
29	H	3	2	1	1.084	121.39	-178.23
30	H	6	5	4	1.088	121.04	-178.67
31	H	11	8	7	1.082	122.27	0.02
32	H	13	12	11	1.083	116.73	-179.94
33	H	14	13	12	1.086	118.17	-179.99
34	H	18	17	10	1.088	120.31	0.10
35	H	19	18	17	1.087	119.96	-179.97
36	H	20	19	18	1.087	119.95	179.94
37	H	21	20	19	1.087	120.02	179.80
38	H	22	21	20	1.088	119.55	179.79
39	H	23	16	2	1.099	108.38	-158.19
40	H	23	16	2	1.094	113.10	-42.90
41	H	24	23	16	1.096	109.77	177.05
42	H	24	23	16	1.096	110.19	-65.31
43	H	25	24	23	1.097	109.09	70.07
44	H	25	24	23	1.096	109.92	-173.00
45	H	26	25	24	1.096	109.54	172.43
46	H	26	25	24	1.097	109.30	-70.50
47	H	27	16	2	1.098	108.47	157.87
48	H	27	16	2	1.092	113.99	41.77

(Table S2 - continued)

Jul-Rosol

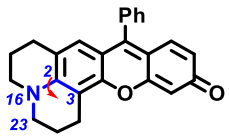

Tag	Symbol	NA	NB	NC	Bond	Angle	Dihedral
1	C						
2	C	1			1.408		
3	C	2	1		1.410	118.13	
4	C	3	2	1	1.412	120.27	-2.07
5	C	4	3	2	1.393	121.63	1.58
6	C	5	4	3	1.400	117.93	-0.42
7	O	4	3	2	1.373	116.90	-178.26
8	C	7	4	3	1.385	119.95	-179.77
9	C	8	7	4	1.471	120.40	-0.12
10	C	9	8	7	1.360	120.37	-0.12
11	C	8	7	4	1.340	118.22	179.89
12	C	11	8	7	1.476	121.13	-180.00
13	C	12	11	8	1.478	117.64	0.12
14	C	13	12	11	1.340	120.64	-0.12
15	O	12	11	8	1.225	121.27	-179.88
16	N	2	1	6	1.396	120.53	-178.05
17	C	10	9	8	1.485	120.21	-179.97
18	C	17	10	9	1.401	120.21	-90.69
19	C	18	17	10	1.396	120.13	-179.80
20	C	19	18	17	1.395	120.03	0.12
21	C	20	19	18	1.395	120.12	0.09
22	C	21	20	19	1.396	120.03	-0.09
23	C	16	2	1	1.459	119.39	172.07
24	C	23	16	2	1.517	110.81	38.13
25	C	3	2	1	1.511	119.97	179.28
26	C	1	6	5	1.510	118.33	-177.37
27	C	26	1	6	1.521	112.21	-166.12
28	C	16	2	1	1.459	118.08	17.14
29	H	6	5	4	1.088	120.32	-179.57
30	H	11	8	7	1.082	122.25	-0.01
31	H	13	12	11	1.083	116.75	179.87
32	H	14	13	12	1.086	118.16	179.95
33	H	18	17	10	1.088	120.30	0.09
34	H	19	18	17	1.087	119.95	-179.99
35	H	20	19	18	1.087	119.94	179.95
36	H	21	20	19	1.087	120.02	179.82
37	H	22	21	20	1.088	119.57	179.79
38	H	23	16	2	1.096	109.76	158.38
39	H	23	16	2	1.097	109.66	-84.10
40	H	24	23	16	1.098	109.82	61.32
41	H	24	23	16	1.095	110.41	179.47
42	H	25	3	2	1.096	110.61	-141.94
43	H	25	3	2	1.097	108.52	99.84
44	H	26	1	6	1.096	110.11	-44.52
45	H	26	1	6	1.097	108.17	72.99
46	H	27	26	1	1.098	109.76	74.44
47	H	27	26	1	1.095	110.03	-167.73
48	H	28	16	2	1.096	110.01	-166.96
49	H	28	16	2	1.097	110.11	75.06

THQ-Rosol

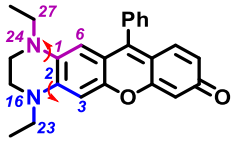

Tag	Symbol	NA	NB	NC	Bond	Angle	Dihedral
1	C						
2	C	1			1.438		
3	C	2	1		1.407	117.82	
4	C	3	2	1	1.396	122.16	0.64
5	C	4	3	2	1.384	121.08	-0.20
6	C	5	4	3	1.404	117.83	-0.13
7	O	4	3	2	1.369	116.31	179.93
8	C	7	4	3	1.387	119.31	-179.84
9	C	8	7	4	1.473	120.34	-0.21
10	C	9	8	7	1.361	120.44	-0.01
11	C	8	7	4	1.340	118.29	179.85
12	C	11	8	7	1.476	121.12	179.96
13	C	12	11	8	1.478	117.65	0.05
14	C	13	12	11	1.340	120.67	-0.06
15	O	12	11	8	1.225	121.27	-179.94
16	N	2	1	6	1.402	121.64	-179.56
17	C	10	9	8	1.485	120.28	-179.84
18	C	17	10	9	1.401	120.22	-90.98
19	C	18	17	10	1.396	120.13	-179.64
20	C	19	18	17	1.395	120.03	0.12
21	C	20	19	18	1.395	120.11	0.10
22	C	21	20	19	1.396	120.03	-0.09
23	C	16	2	1	1.460	124.17	-170.84
24	N	1	6	5	1.427	120.76	179.61
25	C	24	1	6	1.469	111.67	157.20
26	C	16	2	1	1.461	115.95	-9.30
27	C	24	1	6	1.469	119.33	12.21
28	C	27	24	1	1.523	113.62	-173.30
29	C	23	16	2	1.521	110.44	-91.60
30	H	3	2	1	1.085	120.89	-178.64
31	H	6	5	4	1.084	117.41	-179.97
32	H	11	8	7	1.082	122.26	-0.03
33	H	13	12	11	1.083	116.73	179.91
34	H	14	13	12	1.086	118.17	179.94
35	H	18	17	10	1.088	120.30	0.17
36	H	19	18	17	1.087	119.93	-179.99
37	H	20	19	18	1.087	119.93	179.98
38	H	21	20	19	1.087	120.02	179.83
39	H	22	21	20	1.088	119.57	179.75
40	H	23	16	2	1.096	112.10	32.85
41	H	23	16	2	1.098	109.81	149.19
42	H	25	24	1	1.094	111.12	170.53
43	H	25	24	1	1.098	109.95	-70.69
44	H	26	16	2	1.098	109.36	-84.00
45	H	26	16	2	1.097	109.96	158.17
46	H	27	24	1	1.096	109.69	-55.59
47	H	27	24	1	1.097	110.21	63.71
48	H	28	27	24	1.095	109.99	170.45
49	H	28	27	24	1.094	111.57	-70.83
50	H	28	27	24	1.095	111.30	50.61
51	H	29	23	16	1.094	110.27	-178.42
52	H	29	23	16	1.095	110.87	-58.71
53	H	29	23	16	1.094	111.70	61.36

(Table S2 - continued)

N-Methyl-THQ-Rosol

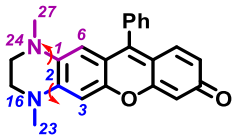

Tag	Symbol	NA	NB	NC	Bond	Angle	Dihedral
1	C						
2	C	1			1.431		
3	C	2	1		1.404	118.21	
4	C	3	2	1	1.397	121.64	-1.09
5	C	4	3	2	1.386	121.17	0.29
6	C	5	4	3	1.404	117.89	0.20
7	O	4	3	2	1.369	116.28	-179.78
8	C	7	4	3	1.387	119.31	179.73
9	C	8	7	4	1.473	120.37	0.20
10	C	9	8	7	1.361	120.47	0.02
11	C	8	7	4	1.340	118.27	-179.85
12	C	11	8	7	1.476	121.12	-179.97
13	C	12	11	8	1.478	117.65	-0.04
14	C	13	12	11	1.340	120.67	0.05
15	O	12	11	8	1.225	121.27	179.96
16	N	2	1	6	1.398	120.96	178.62
17	C	10	9	8	1.485	120.31	179.84
18	C	17	10	9	1.401	120.22	-89.91
19	C	18	17	10	1.396	120.14	-179.75
20	C	19	18	17	1.395	120.03	0.15
21	C	20	19	18	1.395	120.11	0.10
22	C	21	20	19	1.396	120.03	-0.11
23	C	16	2	1	1.448	123.60	169.49
24	N	1	6	5	1.400	120.48	-179.10
25	C	24	1	6	1.463	116.93	169.04
26	C	16	2	1	1.460	116.04	-16.14
27	C	24	1	6	1.450	122.92	-18.24
28	H	3	2	1	1.085	120.59	178.39
29	H	6	5	4	1.085	118.59	-179.22
30	H	11	8	7	1.082	122.26	0.02
31	H	13	12	11	1.083	116.73	-179.94
32	H	14	13	12	1.086	118.17	-179.96
33	H	18	17	10	1.088	120.28	0.14
34	H	19	18	17	1.087	119.95	-179.94
35	H	20	19	18	1.087	119.95	179.96
36	H	21	20	19	1.087	120.04	179.77
37	H	22	21	20	1.088	119.58	179.70
38	H	23	16	2	1.095	111.20	-49.28
39	H	23	16	2	1.095	110.68	72.22
40	H	23	16	2	1.095	111.39	-168.29
41	H	25	24	1	1.096	111.07	159.13
42	H	25	24	1	1.097	108.62	-83.40
43	H	26	16	2	1.097	109.15	-76.87
44	H	26	16	2	1.096	110.94	165.27
45	H	27	24	1	1.095	111.61	-171.96
46	H	27	24	1	1.095	111.01	-52.45
47	H	27	24	1	1.095	110.83	69.11

N-Propyl-THQ-Rosol

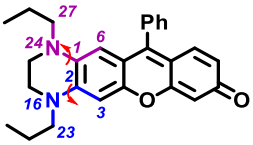

Tag	Symbol	NA	NB	NC	Bond	Angle	Dihedral
1	C						
2	C	1			1.435		
3	C	2	1		1.407	117.80	
4	C	3	2	1	1.397	121.99	2.38
5	C	4	3	2	1.384	121.11	-0.65
6	C	5	4	3	1.403	117.80	-1.01
7	O	4	3	2	1.369	116.35	179.36
8	C	7	4	3	1.387	119.30	-179.77
9	C	8	7	4	1.473	120.36	0.24
10	C	9	8	7	1.360	120.45	-0.36
11	C	8	7	4	1.340	118.28	-179.88
12	C	11	8	7	1.476	121.12	-179.80
13	C	12	11	8	1.478	117.66	0.15
14	C	13	12	11	1.340	120.67	-0.15
15	O	12	11	8	1.225	121.26	-179.95
16	N	2	1	6	1.411	121.31	178.81
17	C	10	9	8	1.485	120.39	179.73
18	C	17	10	9	1.401	120.17	-91.11
19	C	18	17	10	1.396	120.14	-179.45
20	C	19	18	17	1.395	120.02	0.12
21	C	20	19	18	1.395	120.11	0.10
22	C	21	20	19	1.396	120.03	-0.09
23	C	16	2	1	1.464	122.13	-165.45
24	N	1	6	5	1.400	120.37	-177.69
25	C	24	1	6	1.462	116.21	168.09
26	C	16	2	1	1.467	114.25	-16.25
27	C	24	1	6	1.459	125.06	-15.45
28	C	27	24	1	1.529	110.81	-76.37
29	C	23	16	2	1.530	110.04	-94.92
30	C	28	27	24	1.520	111.43	-179.36
31	C	29	23	16	1.520	111.47	179.91
32	H	3	2	1	1.084	120.97	-177.45
33	H	6	5	4	1.084	118.02	-178.40
34	H	11	8	7	1.082	122.26	0.13
35	H	13	12	11	1.083	116.73	179.83
36	H	14	13	12	1.086	118.19	179.95
37	H	18	17	10	1.088	120.29	0.35
38	H	19	18	17	1.087	119.95	-179.99
39	H	20	19	18	1.087	119.95	179.96
40	H	21	20	19	1.087	120.03	179.76
41	H	22	21	20	1.088	119.58	179.61
42	H	23	16	2	1.096	112.04	30.02
43	H	23	16	2	1.098	109.72	146.09
44	H	25	24	1	1.096	110.85	160.58
45	H	25	24	1	1.097	108.90	-81.77
46	H	26	16	2	1.098	109.53	-76.58
47	H	26	16	2	1.097	109.83	165.58
48	H	27	24	1	1.096	111.46	48.11
49	H	27	24	1	1.098	109.53	163.46
50	H	28	27	24	1.097	109.81	-58.11
51	H	28	27	24	1.096	110.56	59.34
52	H	29	23	16	1.097	109.65	-58.99
53	H	29	23	16	1.096	110.71	58.26
54	H	30	28	27	1.094	110.26	179.77
55	H	30	28	27	1.095	110.95	-60.53
56	H	30	28	27	1.095	111.03	60.02
57	H	31	29	23	1.094	110.26	179.62
58	H	31	29	23	1.095	110.96	-60.66
59	H	31	29	23	1.095	111.03	59.88

3. Chemical Synthesis

Chemical shifts (δ) are expressed in ppm, and coupling constants (*J*) in hertz (Hz). Chemical shifts are reported using $CDCl_3$ or the otherwise specified deuterated NMR solvent peak as the internal reference.

General Synthesis A: Friedel-Crafts Acylation. To an oven-dried round bottom flask was added compound **1** (1 eq) and dry CH_2Cl_2 (15 mL). The solution was degassed with N_2 and cooled to 0°C. Benzoyl chloride (1 eq) was added with continuous N_2 bubbling. *$AlCl_3$ (1 eq) was quickly added while maintaining positive N_2 pressure into the flask (color turned bright red). The flask was removed from the ice bath and continued stirring under a blanket of N_2 at room temp for 3 hrs. Dilute HCl (1 M, 4 mL) was added into the reaction flask and stirred for one minute. The reaction mixture was poured into a separatory funnel and the crude material was extracted with DCM (50 mL x 3). The organic fractions were combined, washed with brine, dried over $MgSO_4$, and the solvent removed *in vacuo*. Purification by column chromatography yielded both the acylated phenol intermediate (i.e., compound **2**) and the acylated methoxy-intermediate (not shown) as a byproduct. To preserve starting material **1**, a subsequent demethylation step was performed on the respective acylated methoxy-intermediate to afford additional compound **2**. For efficiently obtaining additional compound **2**, the acylated methoxy-intermediate was demethylated according using the following procedure: The intermediate (1 eq) was added to an oven-dried round bottom flask. The flask was purged with N_2. Then, 5 mL of dry DCM was added. The flask was cooled to -78°C and BBr_3 (1M in DCM, 1.3 eq) was slowly syringed in. The solution turned red. The reaction stirred at -78°C for 2.5 hrs and then at 0°C for 0.5 hrs. 5 mL of cold saturated sodium bicarbonate was slowly syringed into the reaction flask. The flask contents were sonicated and then poured into a separatory funnel. The crude product was extracted with DCM (50 mL x 3). The organic layers were combined, washed with brine, dried over $MgSO_4$, and the solvent removed *in vacuo*. *Note: synthesis of compound **4** from **3** involved 3 eq. of aluminum chloride, which efficiently both acylated and demethylated **3** during the reaction such that a subsequent demethylation of its acylated methoxy-intermediate, as was done for preparing additional compound **2**, was unnecessary.

General Synthesis B: Condensation/Cyclization. Into a small sealed tube was added compound **2** or **4** (1 eq), resorcinol (1.5 eq), and methanesulfonic acid (1 mL). The mixture stirred at 100°C for 3 hrs. The oil was rinsed from the exterior of the tube and 3 mL of DI water was added to the reaction mixture. The red solution turned cloudy. The material was poured into a separatory funnel and extracted with DCM (50 mL x 5). The organic fractions were combined, dried over $MgSO_4$, and the solvent removed *in vacuo.* Purification was performed via column chromatography.

Compound 2-Me. General Synthesis A. The acylated methoxy-intermediate was purified by column chromatography (9:1 hexanes:ethyl acetate) and yielded the product as a yellow solid (223 mg, 33%): ^{1}H NMR (400 MHz, $CDCl_3$) δ (ppm) 7.70-7.75 (m, 2H), 7.45-7.51 (m, 1H), 7.43 (d, 1H, *J* = 8.7 Hz), 7.36-7.43 (m, 2H), 6.30 (dd, 1H, *J* = 2.3, 8.7 Hz), 6.16 (d, 1H, *J* = 2.3 Hz), 3.72 (s, 3H), 3.06 (s, 6H); ^{13}C NMR (125 MHz, $CDCl_3$) δ (ppm) 195.3, 160.7, 154.3, 140.4, 133.7, 131.6, 129.6, 127.9. HRMS calculated for $C_{16}H_{17}NO_2Na$ (M + Na^+): 278.1152. Found: 278.1149. Compound **2-Me** was purified by column chromatography (9:1 hexanes:ethyl acetate) yielded the product as a yellow oil (209 mg, 89%): ^{1}H NMR (400 MHz, $CDCl_3$) δ (ppm) 12.96 (s, 1H), 7.57-7.63 (m, 2H), 7.48-7.53 (m, 1H), 7.42-7.48 (m, 2H), 7.36-7.41 (m, 1H), 6.13-6.18 (m, 2H), 3.04 (s, 6H); ^{13}C NMR (125 MHz, $CDCl_3$) δ (ppm) 198.3, 165.9, 155.9, 138.9, 135.3, 130.8, 128.7, 128.2, 109.3, 103.8, 97.9, 40.0. HRMS calculated for $C_{15}H_{16}NO_2$ (M + H^+): 242.1176. Found: 242.1177.

Me-Rosol. General Synthesis B. Purification via column chromatography (9:1 DCM:ethyl acetate) yielded the product as a red solid (131 mg, 69%): ^{1}H NMR (400 MHz, $CDCl_3$) δ (ppm) 7.51-7.57 (m, 3H), 7.27-7.33 (m, 2H), 7.00-7.06 (m, 2H), 6.49-6.55 (m, 3H), 6.38 (d, 1H, *J* = 2.0 Hz), 3.10 (s, 6H); ^{13}C NMR (125 MHz, $CDCl_3$) δ (ppm) 184.9, 159.1, 155.3, 154.1, 150.8, 133.2, 130.7, 129.8, 129.4, 129.3, 128.6, 128.0, 115.0, 110.7, 110.0, 105.2, 96.9, 40.2. HRMS calculated for $C_{21}H_{18}NO_2$ (M + H^+): 316.1332. Found: 316.1329.

Compound 2-Et. General Synthesis A. The acylated methoxy-intermediate was purified by column chromatography (9:1 hexanes:ethyl acetate) and yielded the product as a yellow oil (168 mg, 35%): ^{1}H NMR (400 MHz, $CDCl_3$) δ (ppm) 7.71-7.75 (m, 2H), 7.44-7.49 (m, 1H), 7.42 (d, 1H, *J* = 8.8 Hz), 7.36-7.41 (m, 2H), 6.26 (dd, 1H, *J* = 2.4, 8.8 Hz), 6.14 (d, 1H, *J* = 2.4 Hz), 3.70 (s, 3H), 3.42 (q, 4H, *J* = 7.1 Hz), 1.22 (t, 6H, *J* = 7.1 Hz); ^{13}C NMR (125 MHz, $CDCl_3$) δ (ppm) 195.0, 161.2, 152.0, 140.6, 134.2, 131.3, 129.5, 127.8, 115.4, 103.4, 94.2, 55.5, 44.7, 12.7. HRMS calculated for $C_{18}H_{21}NO_2Na$ (M + Na^+): 306.1465. Found: 306.1462. Compound **2-Et** was purified via column chromatography (1:1 DCM:hexanes) and yielded the

product as a yellow oil (295 mg, 92%): ^{1}H NMR (400 MHz, $CDCl_3$) δ (ppm) 13.03 (s, 1H), 7.58-7.63 (m, 2H), 7.42-7.53 (m, 3H), 7.37 (d, 1H, *J* = 9.1 Hz), 6.12-6.17 (m, 2H), 3.39 (q, 4H, *J* = 7.1 Hz), 1.20 (t, 6H, *J* = 7.1 Hz); ^{13}C NMR (125 MHz, $CDCl_3$) δ (ppm) 197.9, 166.3, 153.9, 139.0, 135.6, 130.7, 128.7, 128.2, 108.9, 103.6, 97.2, 44.7, 12.7. HRMS calculated for $C_{17}H_{19}NO_2Na$ (M + Na^+): 292.1308. Found: 292.1309.

Et-Rosol. General Synthesis B. Purification by column chromatography (9:1 DCM:ethyl acetate) yielded the product as a red solid (11.4 mg, 8%): ^{1}H NMR (400 MHz, MeOD) δ (ppm) 7.60-7.66 (m, 3H), 7.38-7.44 (m, 2H), 7.20 (d, 1H, *J* = 9.4 Hz), 7.16 (d, 1H, *J* = 9.5 Hz), 6.87 (dd, 1H, *J* = 2.5 Hz, 9.4 Hz), 6.81 (d, 1H, *J* = 2.5 Hz), 6.56 (dd, 1H, *J* = 2.2 Hz, 9.5 Hz), 6.48 (d, 1H, *J* = 2.2 Hz), 3.59 (q, 4H, *J* = 7.1 Hz), 1.26 (t, 6H, *J* = 7.1 Hz); ^{13}C NMR (125 MHz, MeOD) δ (ppm) 185.2, 161.1, 158.2, 156.5, 155.4, 134.3, 132.7, 132.1, 130.8, 130.6, 129.8, 126.5, 114.8, 113.3, 112.4, 105.0, 97.3, 46.3, 12.8. HRMS calculated for $C_{23}H_{21}NO_2$ (M + H^+): 344.1645. Found: 344.1642.

Compound 2-Pip. General Synthesis A. The acylated methoxy-intermediate was purified by column chromatography (9:1 hexanes:ethyl acetate) and yielded the product as a yellow oil (54 mg, 15%): ^{1}H NMR (400 MHz, $CDCl_3$) δ (ppm) 7.73-7.77 (m, 2H), 7.46-7.52 (m, 1H), 7.36-7.42 (m, 2H), 7.39 (d, 1H, *J* = 8.6 Hz), 6.50 (dd, 1H, *J* = 2.3, 8.6 Hz), 6.40 (d, 1H, *J* = 2.3 Hz), 3.70 (s, 3H), 3.29-3.36 (m, 4H), 1.60-1.75 (m, 6H). ^{13}C NMR (125 MHz, $CDCl_3$) δ (ppm) 195.3, 160.4, 155.5, 140.0, 133.1, 131.8, 129.7, 127.9, 118.3, 106.8, 98.2, 55.6, 49.4, 25.7, 24.5. HRMS calculated for $C_{19}H_{21}NO_2Na$ (M + Na^+): 318.1465. Found: 318.1465. Compound **2-Pip** was purified via column chromatography (9:1 hexanes:EtOAc) and yielded the product as a yellow oil (129 mg, 94%): ^{1}H NMR (400 MHz, $CDCl_3$) δ (ppm) 12.85 (s, 1H), 7.59-7.63 (m, 2H), 7.50-7.55 (m, 1H), 7.44-7.49 (m, 2H), 7.39 (d, 1H, *J* = 9.1 Hz), 6.35 (d, 1H, *J* = 2.6 Hz), 6.31 (dd, 1H, *J* = 2.6, 9.1 Hz), 3.38-3.44 (m, 4H), 1.60-1.71 (m, 6H); ^{13}C NMR (125 MHz, $CDCl_3$) δ (ppm) 198.3, 166.3, 156.3, 138.3, 135.4, 131.0, 128.8, 128.3, 109.9, 105.3, 99.7, 48.2, 25.4, 24.6; HRMS calculated for $C_{18}H_{19}NO_2Na$ (M + Na^+): 304.1308. Found: 304.1309.

Pip-Rosol. General Synthesis B. Purification via column chromatography (9:1 DCM:MeOH) yielded the product as a red solid (41 mg, 25%): ^{1}H NMR (400 MHz, $CDCl_3$) δ (ppm) 7.49-7.56 (m, 3H), 7.28-7.34 (m, 2H), 7.00-7.07 (m, 2H), 6.73 (d, 1H *J* = 2.5 Hz), 6.69 (dd, 1H, *J* = 2.5, 9.1 Hz), 6.53 (dd, 1H, *J* = 2.0, 9.6 Hz), 6.42 (d, 1H, *J* = 2.0 Hz), 3.38-3.51 (m, 4H), 1.58-1.75 (m, 6H); ^{13}C NMR (125 MHz, $CDCl_3$) δ (ppm) 185.1, 159.2, 155.7, 154.5, 150.6, 133.3, 130.9, 130.0, 129.5, 129.3, 128.6, 128.3, 115.6, 111.6, 111.4, 105.3, 98.8, 48.5, 25.4, 24.4. HRMS calculated for $C_{24}H_{21}NO_2$ (M + H^+): 356.1645. Found: 356.1643.

Compound 2-Jul. General Synthesis A. The acylated methoxy-intermediate was purified by column chromatography (9:1 hexanes:EtOAc) and yielded the product as a yellow oil (249 mg, 33%): ^{1}H NMR (400 MHz, $CDCl_3$) δ (ppm) 7.75-7.81 (m, 2H), 7.46-7.53 (m, 1H), 7.37-7.44 (m, 2H), 7.02 (s, 1H), 3.51 (s, 3H), 3.20-3.27 (m, 4H), 2.76 (t, 2H, *J* = 6.5 Hz), 2.69 (t, 2H, J = 6.4 Hz), 1.91-1.99 (m, 4H); ^{13}C NMR (125 MHz, $CDCl_3$) δ (ppm) 195.5, 157.0, 147.0, 140.1, 131.7, 130.3, 129.8, 127.9, 118.4, 115.9, 113.5, 61.6, 50.1, 49.7, 27.5, 21.8, 21.3, 21.3. HRMS calculated for $C_{20}H_{21}NO_2Na$ (M + Na^+): 330.1465. Found: 330.1462. Compound **2-Jul** was purified via column chromatography (9:1 hexanes:EtOAc) and yielded the product as a yellow oil (25.8 mg, 27%): ^{1}H NMR (400 MHz, $CDCl_3$) δ (ppm) 13.27 (s, 1H), 7.56-7.60 (m, 2H), 7.42-7.52 (m, 3H), 6.95 (s, 1H), 3.23-3.31 (m, 4H, *J* = 5.8 Hz), 2.75 (t, 2H, *J* = 6.4 Hz), 2.57 (t, 2H, *J* = 6.3 Hz), 1.87-2.00 (m, 4H); ^{13}C NMR (125 MHz, $CDCl_3$) δ (ppm) 197.8, 161.5, 149.2, 139.5, 131.3, 130.4, 128.7, 128.2, 112.6, 108.4, 105.9, 50.3, 49.9, 27.5, 21.9, 20.9, 20.1. HRMS calculated for $C_{19}H_{19}NO_2Na$ (M + Na^+): 316.1308. Found: 316.1308.

Jul-Rosol. General Synthesis B. Purification of the crude material via column chromatography (10:1 DCM:MeOH) yielded the product as a dark red solid (4.7 mg, 4%): ^{1}H NMR (400 MHz, MeOD) δ (ppm) 7.60-7.66 (m, 1H), 7.35-7.42 (m, 2H), 7.16 (d, 1H, *J* = 8.0 Hz), 6.84 (s, 1H), 6.62-6.67 (m, 2H), 3.46-3.57 (m, 4H), 3.02 (t, 2H, *J* = 6.4 Hz), 2.68 (t, 2H, *J* = 6.4 Hz), 2.07 (qn, 2H, *J* = 6.0 Hz); ^{13}C NMR (125 MHz, $CDCl_3$) δ (ppm) 160.0, 156.5, 153.6, 152.5, 134.3, 132.3, 130.8, 130.6, 129.8, 127.9, 125.0, 123.8, 114.2, 113.7, 106.6, 104.4, 51.9, 51.4, 28.6, 21.8, 20.8. HRMS calculated for $C_{25}H_{21}NO_2$ (M + H^+): 368.1645. Found: 368.1641.

Compound 4. General Synthesis A. Purification via column chromatography (8:2 hexanes:EtOAc) yielded the product as a yellow solid (203 mg, 48%): ^{1}H NMR (400 MHz, $CDCl_3$) δ (ppm) 12.94 (s, 1H), 7.61-7.66 (m, 2H), 7.42 -7.52 (m, 3H), 6.59 (s, 1H), 6.13 (s, 1H), 3.47-3.53 (m, 2H), 3.40 (q, 2H, *J* = 7.1 Hz), 3.09-3.13 (m, 2H), 3.06 (q, 2H, *J* = 7.1 Hz), 1.22 (t, 3H, *J* = 7.1 Hz), 1.06 (t, 3H, *J* = 7.1 Hz); ^{13}C NMR (125 MHz, $CDCl_3$) δ (ppm) 197.2, 161.2, 144.5, 139.4, 130.5, 128.6, 128.0,

127.1, 113.8, 108.1, 96.4, 47.8, 45.7, 45.4, 45.0, 10.7, 10.1. HRMS calculated for $C_{19}H_{22}N_2O_2$ (M^+): 309.1598. Found: 309.1597.

THQ-Rosol. General Synthesis B. Purification via column chromatography (9:1 $CHCl_3$:MeOH) yielded the product as a yellow oil (49%): ^{1}H NMR (400 MHz, $CDCl_3$) δ (ppm) 7.49-7.55 (m, 3H), 7.28-7.34 (m, 2H), 7.03 (d, 1H, *J* = 9.6 Hz), 6.58 (dd, 1H, *J* = 2.1, 9.6 Hz), 6.52 (s, 1H), 6.48 (d, 1H *J* = 2.1 Hz), 6.10 (s, 1H), 3.51-3.56 (m, 2H), 3.47 (q, 2H, *J* = 7.2 Hz), 3.16-3.21 (m, 2H), 3.04 (q, 2H, *J* = 7.1 Hz), 1.25 (t, 3H, *J* = 7.2 Hz), 0.96 (t, 3H, *J* = 7.1 Hz); ^{13}C NMR (125 MHz, $CDCl_3$) δ (ppm) 183.6, 158.9, 151.1, 150.4, 143.3, 134.0, 132.7, 130.0, 129.4, 129.2, 128.5, 127.5, 114.5, 111.5, 105.9, 104.4, 95.3, 47.7, 46.4, 45.4, 44.6, 10.8, 9.6. HRMS calculated for $C_{25}H_{24}N_2O_2$ ($M + H^+$): 385.1911. Found: 385.1910.

4. UV/Vis & Fluorescence Spectroscopy

Spectroscopy. The PTI Quantamaster 400 (QM-400) spectrofluorometer is equipped with an extended wavelength range (185-900 nm) Shimadzu 928 photomultiplier tube (PMT), a 1200 l/mm grating blazed at 500 nm, and an OBB PowerArc™ 75W Xenon arc lamp (~7500 mW total power output), wherein data was collected using the proprietary PTI *FelixGX©* 4.3.6904.8391 software package. To prepare dye solutions, an appropriate volume of a 1 mg/mL DMSO stock dye solution of each non-NIR fluorescent rosol dye and **THQ-Rosol** was diluted to volume with buffer (50 mM phosphate, 150 mM NaCl, pH 7.4) after addition of negligible volume of co-solvent (DMSO), if needed. Fluorescence spectra of each rosol dye were obtained by exciting each fluorescent rosol dye solution (at 25°C) at their respective wavelength of maximum absorbance and the resultant emission was collected from +10 nm beyond the respective excitation wavelength to 900 nm. The emission spectra of a buffer blank for each fluorescent dye was obtained and automatically subtracted from its respective emission spectrum to account for any Raman scattering and noise from the buffer, wherein the excitation and emission background subtraction feature provided in the software was enabled to account for both any differences in the varying quantum efficiency of the lamp source at each respective excitation wavelength and any dark noise from the PMT upon monitoring the fluorescence emission.

Photostability. Photostability studies on the fluorescent rosol dyes were performed by photoirradiating solutions of each dye for 1800 s at their respective wavelength of maximum absorbance and measuring the fluorescence intensity at their respective wavelength of maximum emission. 2 points per second were obtained without pause.

Quantum Yield. The quantum yields of fluorescence (Φ_{fl}) were determined by using erythrosine B as a reference fluorescent dye (Φ_{fl} = 0.02). Quantum yields were calculated using Eq. S1. The excitation wavelength was 515 nm (with 2 nm excitation and emission slits), wherein the absorbance at 515 nm was less than 0.1 for each fluorescent rosol dye and erythrosine B.[1]

$$\Phi_S = \Phi_R \left[\frac{I_S}{I_R}\right]\left[\frac{A_R}{A_S}\right]\left[\frac{(\eta_S)^2}{(\eta_R)^2}\right] \qquad \text{(Eq. S1)}$$

Φ_S = relative quantum yield of sample
Φ_R = absolute quantum yield of reference fluorescent dye
η_S = refractive index of the sample solvent
η_R = refractive index of the reference solvent
A_S = absorbance of sample
A_R = absorbance of reference fluorescence dye
I_S = fluorescence intensity of sample
I_R = fluorescence intensity of reference fluorescent dye

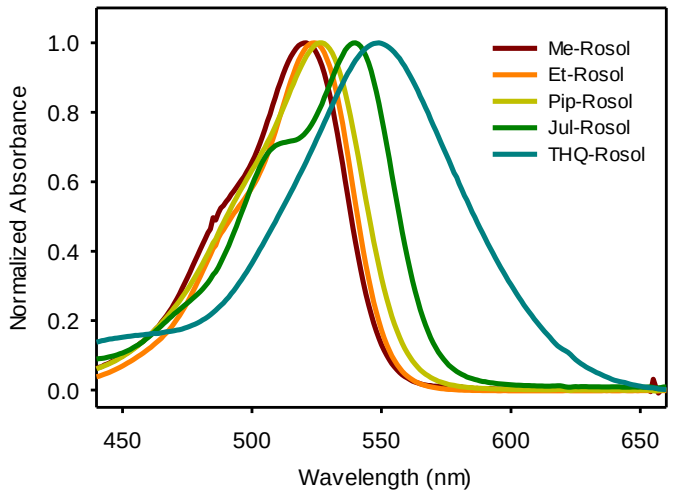

Figure S3. Absorption Spectra. Normalized absorbance spectra of fluorescent rosol dyes (20 µM) in buffer (50 mM phosphate, 150 mM NaCl, pH 7.4).

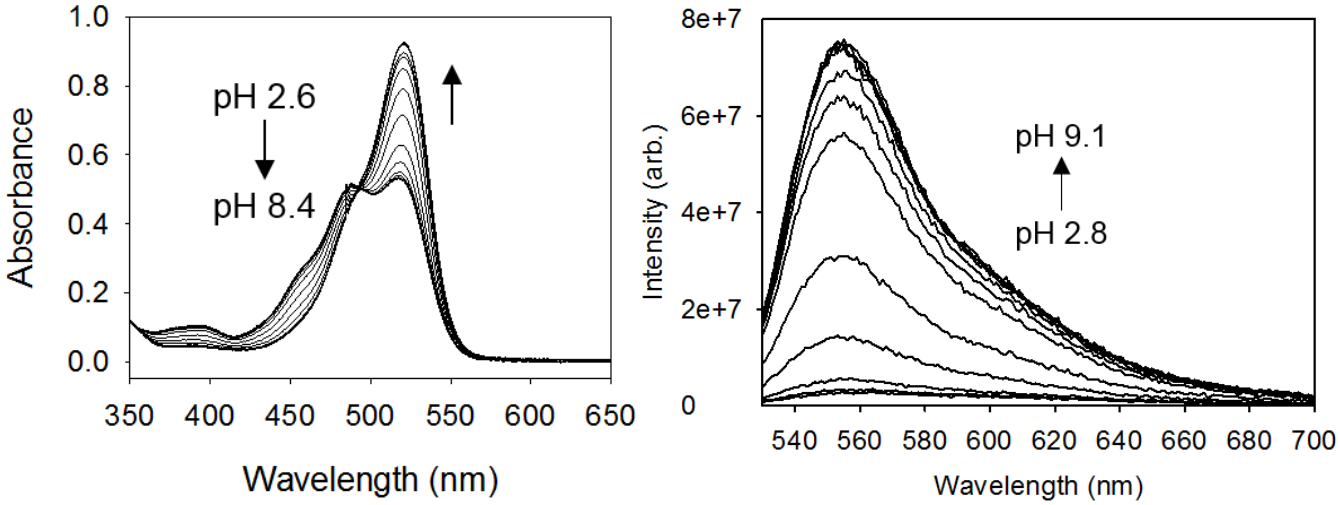

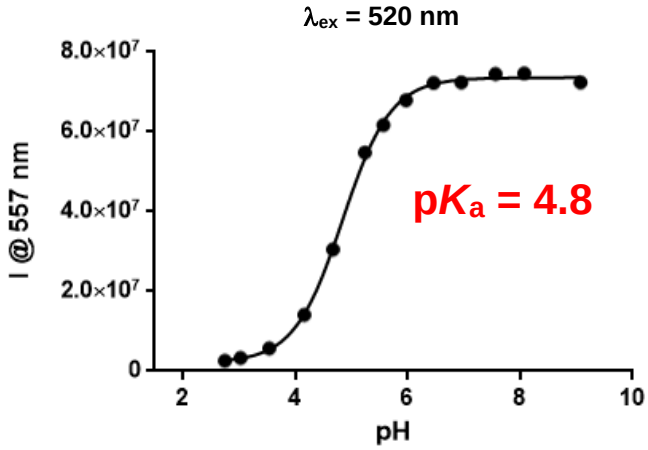

Figure S4. pH Titration of Me-Rosol (20 µM) in buffer (50 mM phosphate, 150 mM NaCl, pH 7.4). Various aliquot volumes of different NaOH solutions having a concentration of either 1, 4, or 8 M were added to the non-NIR fluorescent rosol dye to adjust the pH. A plot of the pH versus the intensity produces a sigmoidal curve where the inflection point represents the pK_a. The non-NIR fluorescent rosol dye was excited at its maximum absorbance wavelength (λ_{abs} = 520 nm).

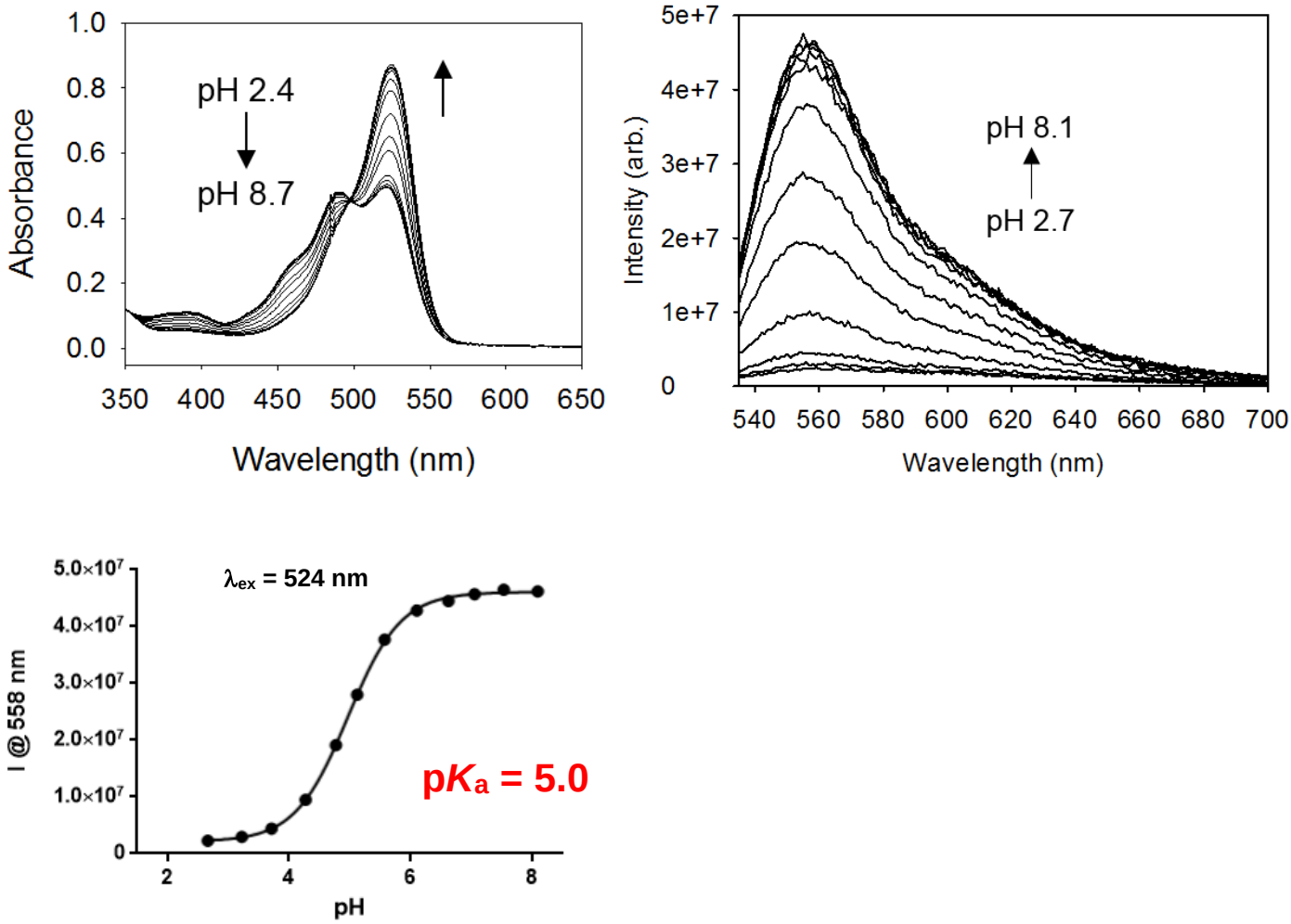

Figure S5. pH Titration of Et-Rosol (20 μM) in buffer (50 mM phosphate, 150 mM NaCl, pH 7.4). Various aliquot volumes of different NaOH solutions having a concentration of either 1, 4, or 8 M were added to the non-NIR fluorescent rosol dye to adjust the pH. A plot of the pH versus the intensity produces a sigmoidal curve where the inflection point represents the pK_a. The non-NIR fluorescent rosol dye was excited at its maximum absorbance wavelength (λ_{abs} = 524 nm).

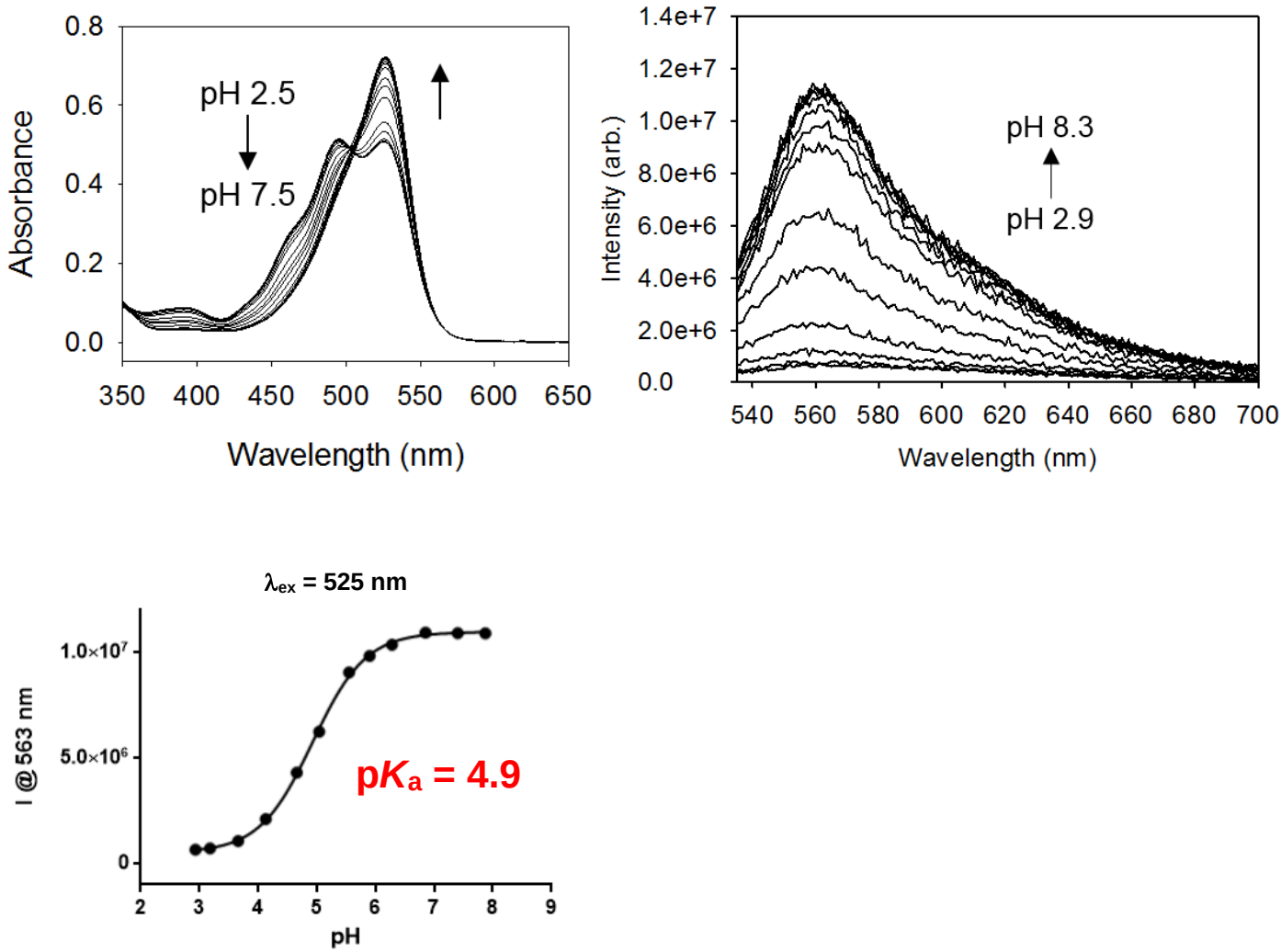

Figure S6. pH Titration of Pip-Rosol (20 μM) in buffer (50 mM phosphate, 150 mM NaCl, pH 7.4). Various aliquot volumes of different NaOH solutions having a concentration of either 1, 4, or 8 M were added to the non-NIR fluorescent rosol dye to adjust the pH. A plot of the pH versus the intensity produces a sigmoidal curve where the inflection point represents the pK_a. The non-NIR fluorescent rosol dye was excited at its maximum absorbance wavelength (λ_{abs} = 525 nm).

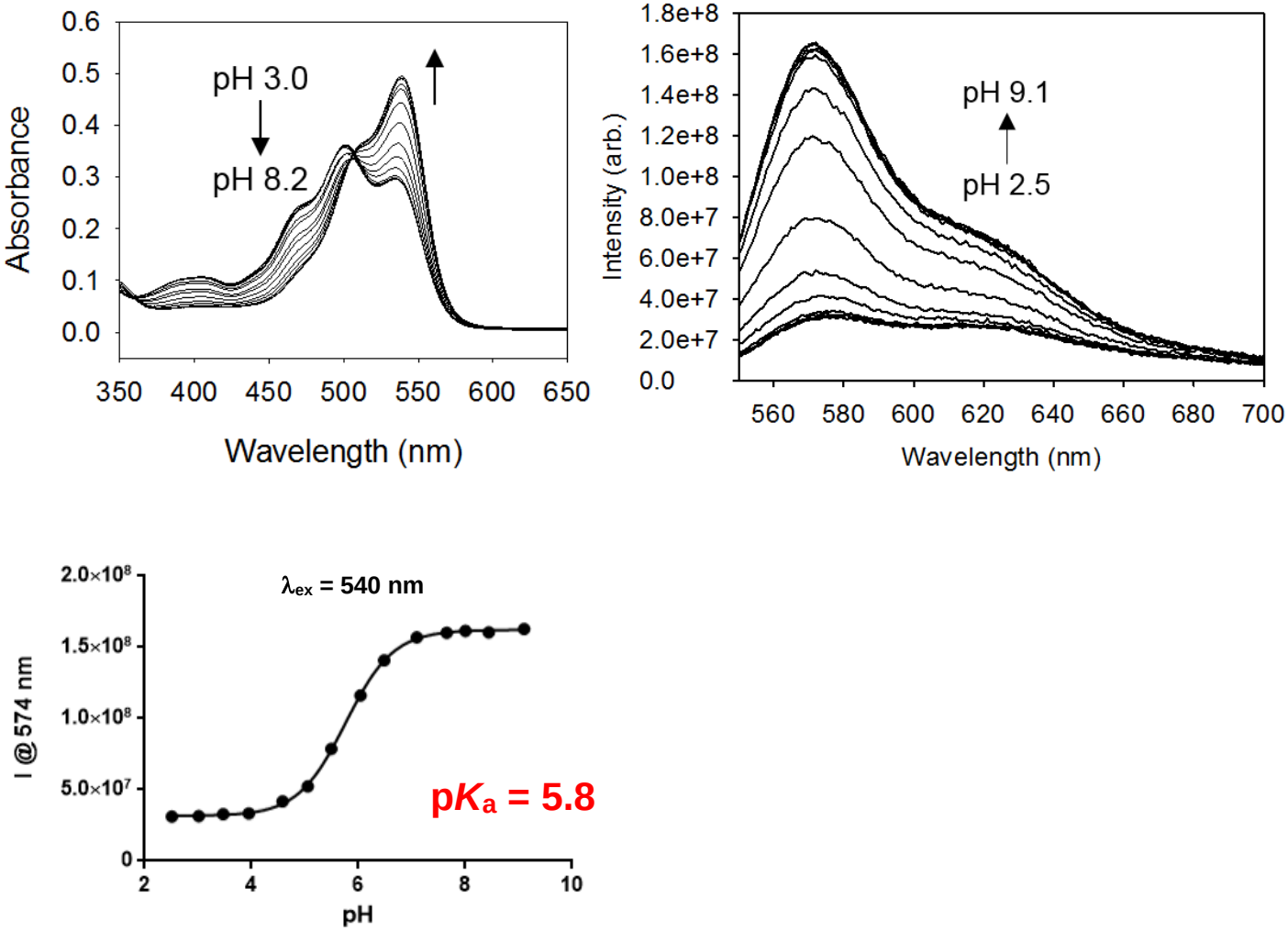

Figure S7. pH Titration of Jul-Rosol (20 μM) in buffer (50 mM phosphate, 150 mM NaCl, pH 7.4). Various aliquot volumes of different NaOH solutions having a concentration of either 1, 4, or 8 M were added to the non-NIR fluorescent rosol dye to adjust the pH. A plot of the pH versus the intensity produces a sigmoidal curve where the inflection point represents the pK_a. The non-NIR fluorescent rosol dye was excited at its maximum absorbance wavelength (λ_{abs} = 540 nm).

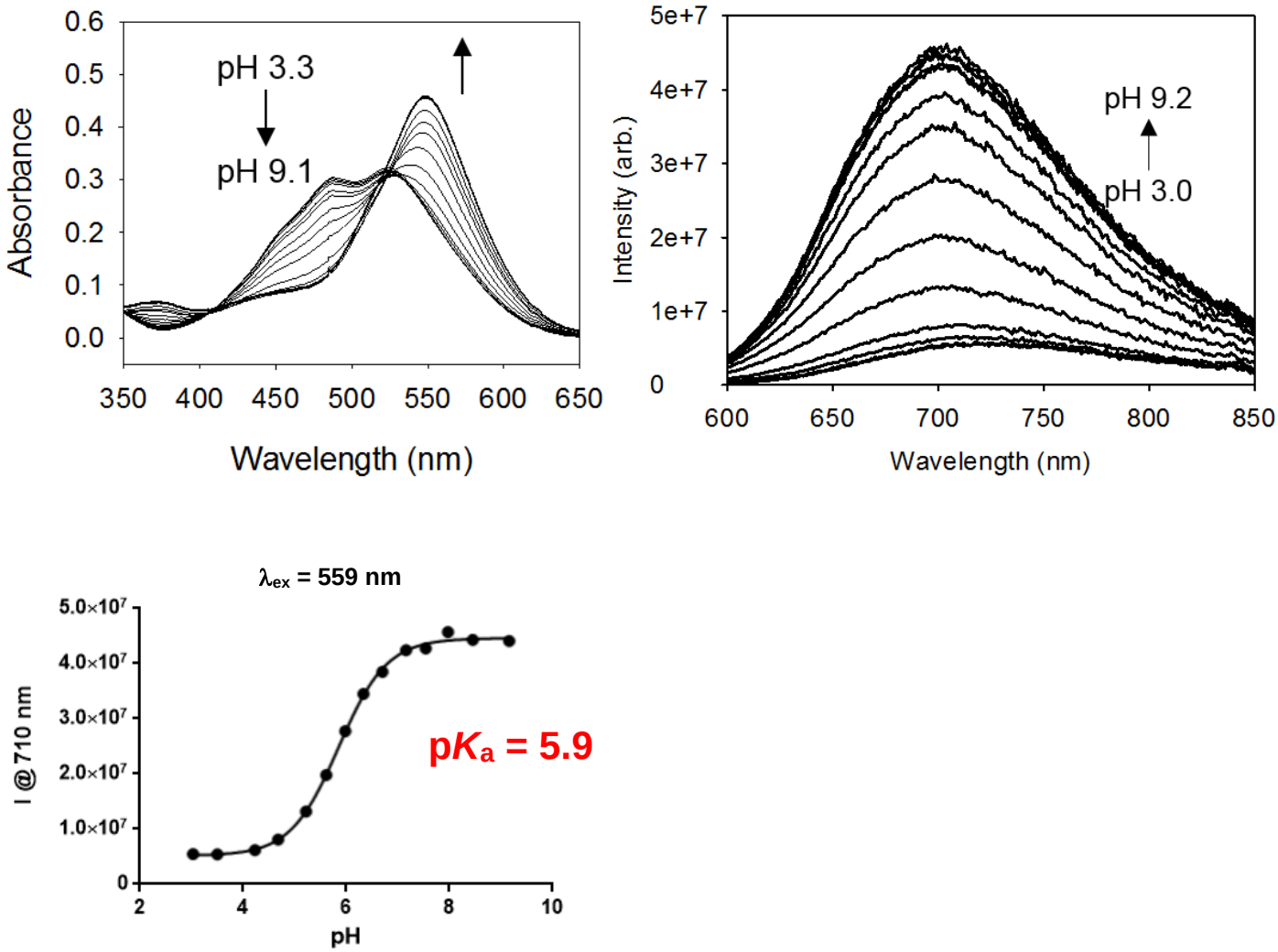

Figure S8. pH Titration of THQ-Rosol (20 μM) in buffer (50 mM phosphate, 150 mM NaCl, pH 7.4). Various aliquot volumes of different NaOH solutions having a concentration of either 1, 4, or 8 M were added to the NIR fluorescent rosol dye to adjust the pH. A plot of the pH versus the intensity produces a sigmoidal curve where the inflection point represents the pK_a. The NIR fluorescent rosol dye was excited at its maximum absorbance wavelength (λ_{abs} = 559 nm).

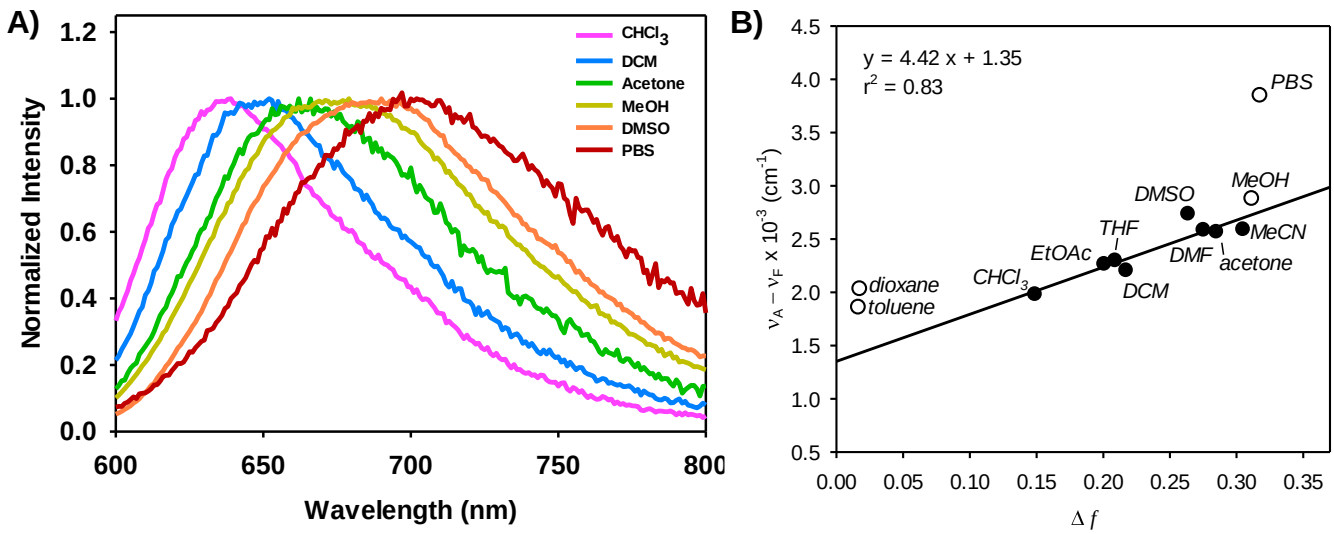

Figure S9. Solvatochromatic Shifts. Solvatochromatic shifts of **THQ-Rosol** (20 µM). A) Normalized fluorescence emission spectra in select solvents. B) Lippert-Mataga correlation plot. A filled dot (●) represents a solvent utilized in constructing a best linear fit to the data, whereas an open dot (○) represents a solvent excluded for doing so due to second-order effects (i.e., specific chemical interactions) that are not described by the Lippert-Mitaga theory, which include H-bonding (MeOH and PBS), π-stacking (toluene), and/or conformational changes (1,4-dioxane). $\nu_A - \nu_F$ is the Stokes shift of **THQ-Rosol** in each solvent and Δf is the orientation polarizability of each solvent, which accounts for both the dielectric constant and refractive index of the solvent. A positive slope alongside a high correlation between the evaluated parameters ($r^2 \geq 0.64$) reveals that the different Stokes shift of **THQ-Rosol** when in a polar aprotic solvent can be attributed to *general solvent effects*, and thus directly proportional to the change in its dipole moment, as described by the Lippert-Mataga theory.[2-6]

Table S3. Absorbance and emission maxima of **THQ-Rosol** (20 µM) evaluated in various solvents.

Solvent	PBS	MeOH	Acetone	Ethyl acetate	DCM	$CHCl_3$	DMF	DMSO	Toluene	1,4-Dioxane	THF	MeCN
λ_{abs} **(nm)**	559	568	568	562	567	568	574	579	562	562	564	568
λ_{em} **(nm)**	710	678	665	644	648	640	674	688	628	638	648	666

Abbreviations: MeOH = methanol, DCM = dichloromethane, $CHCl_3$ = chloroform, DMF = N,N-dimethylformamide, DMSO = dimethyl sulfoxide, THF = tetrahydrofuran, MeCN = acetonitrile, λ_{abs} = maximum absorbance wavelength. λ_{em} = maximum emission wavelength.

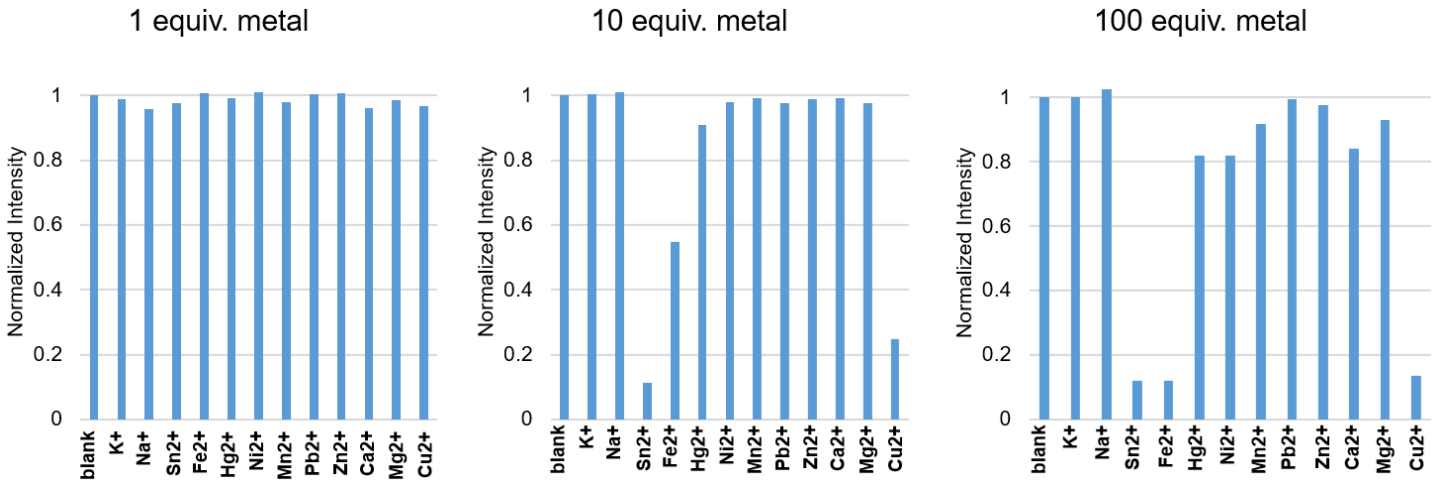

Figure S10. Bioanalyte Titrations. Titration of **THQ-Rosol** (20 µM) with various concentrations of various bioanalytes. The metal salts used for titrations include: $CuCl_2$, $MgCl_2$, $MnCl_2$, NaOAc, KOAc, $SnCl_2$, $Zn(OAc)_2$, $Hg(OAc)_2$, $Pb(OAc)_2$, $NiCl_2$, $CaCl_2$, and $FeCl_2$.

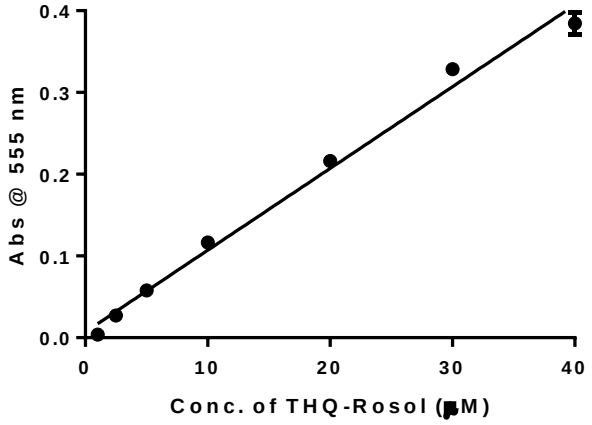

$r^2 = 0.986$

Conc. (µM)	Trial 1	Trial 2	Trial 3
1.0	0.001882	0.001291	0.008195
2.5	0.019889	0.026573	0.034930
5.0	0.056087	0.059930	0.057211
10.0	0.114321	0.116683	0.118048
20.0	0.226612	0.214521	0.207740
30.0	0.315120	0.330655	0.340119
40.0	0.400101	0.356846	0.396193

Figure S11. **Absorption-Based Linearity Profile.** Linearity of **THQ-Rosol** absorbance at different concentrations in PBS buffer, pH 7.4.

5. Cellular Analyses

Cell Culture. GBM U251 cells were cultured in RPMI media and GBM U87 cells were cultured in DMEM, each supplemented with 10% fetal bovine serum, 100 U/mL penicillin, and 100 µg/mL streptomycin. We acknowledge Dr. Sanjiv Sam Gambhir for having gifted the GBM39 cells to us after obtaining them from Dr. Paul Mischel (Ludwig Institute for Cancer Research, University of California at San Diego). The GBM39 cells had been transfected with lentiviral vectors that express firefly luciferase to enable bioluminescence imaging. GBM39 cells were grown in a defined, serum-free media of a 1:1 mixture of Neurobasal-A Medium (1X)/DMEM/F12(1X) that also contained HEPES Buffer Solution (10 mM), MEM Sodium Pyruvate Solution (1 mM), MEM Non-Essential Amino Acids Solution (10 mM, 1X), GlutaMAX-I™ Supplement (1X) and Antibiotic–Antimycotic (1X). All solutions were purchased from Invitrogen™/Life Technologies Inc. The full working media also contained h-EGF (20 ng/mL), h-FGF-basic-154 (20 ng/mL), h-PDGF-AA (10 ng/mL), h-PDGF-BB (10 ng/mL) and heparin solution, 0.2 % (2 µg/mL) as growth factors (all from Shenandoah Inc.) and B-27 (Invitrogen™/Life Technologies) as supplements. All cells were propagated at 37°C in a humidified atmosphere containing 5% CO_2.

Cell Viability Assay. The toxicity of **THQ-Rosol** to cells was evaluated by using Invitrogen™ Calcein-AM to stain live cells (see Supp Info). GBM U251 cells were seeded in a 96-well plate at a density of 10,000 cells per well in DMEM with 10% fetal bovine serum (FBS) and 1% penicillin/streptomycin at 37°C and 5% CO_2. The cells were incubated with **THQ-Rosol** at different concentrations (200 nM, 1 µM, 5 µM, 10 µM, and 25 µM) in several replicates (n = 5) for 2 hours at 37°C. The cells were then incubated with Invitrogen™ Calcein-AM (5 µM) for 45 min at 37°C, and then imaged using a Tecan Safire plate reader with excitation and emission wavelengths of 494 nm and 516 nm, respectively.

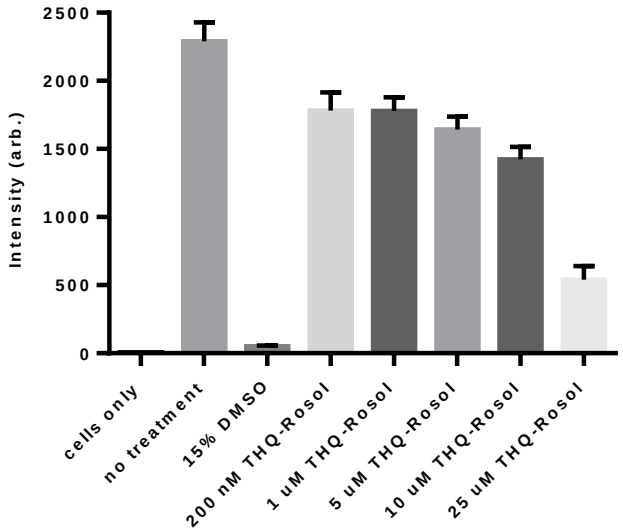

Figure S12. Cell viability assay of THQ-Rosol with U251 GBM cells. The cells were treated with various concentrations of **THQ-Rosol** and then incubated with Invitrogen™ Calcein-AM to determine the extent of live cells via measuring the fluorescence emission at 515 nm (λ_{ex} = 494 nm).

Confocal Microscopy. The cell permeability and localization of **THQ-Rosol** were examined in GBM U87 cells using a Leica SP8 confocal fluorescence microscope. Cells were plated onto 35 mm, 4-chamber glass-bottom dishes (In Vitro Scientific, Inc.) at a density of 50,000 cells/well and allowed to adhere overnight at 37°C in a humidified atmosphere containing 5% CO_2. For assessing the cell permeability of **THQ-Rosol** and its presence within cells, we incubated only **THQ-Rosol** (10 µM, 37°C, 30 min) in GBM U87 cells and then visualized **THQ-Rosol** in the cells (λ_{ex} = 550 nm, λ_{em} = 680-900 nm). To validate **THQ-Rosol** localized to lysosomes, GBM U87 cells were incubated with LysoTracker Green DND-26 (5 µM, 37°C, 30 min), washed with PBS (600 µL), provided DMEM (600 µL, without phenol red), incubated with **THQ-Rosol** (10 µM, 37°C, 30 min), and then imaged to prevent the loss of localized **THQ-Rosol**, wherein we used two different pairs of appropriate excitation and emission channels (λ_{ex1} = 550 nm, λ_{em1} = 680-900 nm for visualizing **THQ-Rosol** and λ_{ex2} = 504 nm, λ_{em2} = 514-530 nm for visualizing LysoTracker Green DND-26). A 100X (NA = 1.40 oil) objective lens was used. Pearson's coefficient was calculated using the Fiji (ImageJ) plugin Coloc 2.

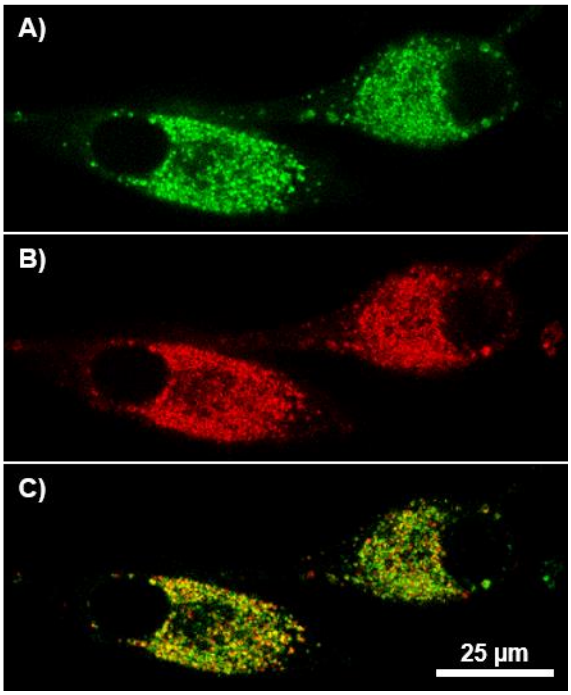

Figure S13. Confocal fluorescence imaging. GBM U87 cells incubated with LysoTracker Green DND-26 (5 µM), incubated with **THQ-Rosol** (10 µM), and visualized using a A) 514-530 nm (λ_{ex1}: 504 nm) band-pass filter for LysoTracker Green DND-26 and B) 680-900 nm (λ_{ex2}: 550 nm) band-pass filter for **THQ-Rosol**, respectively. C) Merged image. Scale bar = 25 µm.

6. *In Vivo* Studies

***In Vivo* Tumor Models.** All experimental procedures involving animals were approved by the Stanford University Institutional Animal Care and Use Committee (IACUC). For tumor models, GBM39 cells (0.5×10^6 cells; 150 µL of serum-free media) were subcutaneously injected on the back of female nu/nu mice (age 17-18 weeks; Charles River Laboratories) and allowed to grow for 6 weeks. Tumor size was monitored by calipers and firefly luciferase bioluminescence imaging.

Animal Imaging. Animals were anesthetized with 2% isoflurane in oxygen and kept on a heating pad between imaging time points, wherein their body temperatures were kept constant at 37°C during imaging. Bioluminescence imaging was obtained via intraperitoneal injections into the mice using firefly D-luciferin (150 µL, 15 mg/mL in PBS), waiting 10 min, and then imaging using exposure time of 300 ms in order to monitor initial tumor growth. Fluorescence imaging was obtained both before after administering either ICG or **THQ-Rosol** (50 µL, 25 µM in 0.9% w/v saline using a 1% w/v DMSO co-solvent) to the mice. The mice were imaged at several time points (0, 0.25, 0.5, 1, 2, 4, 6, 24 hrs) before and following the administration of either dye. Fluorescence images were taken on a Cambridge Research & Instrumentation, Inc. (CRi Inc.) Maestro™ spectral fluorescent imager using a 503-555 nm excitation filter and 580 nm long-pass emission filter for spectral cube images and 710 nm for mono-emission image capture. Spectral unmixing was used to isolate **THQ-Rosol** signal from background. For ICG, we utilized a 710-760 nm band-pass excitation filter and 800 nm long-pass emission filter. Using ImageJ (National Institutes of Health, USA), regions of interest of identical size and shape were manually drawn to separately circumscribe the tumor area and healthy tissue within each image, separately averaged, and presented as a normalized tumor-to-background ratio.

7. ^{1}H & ^{13}C NMR Spectroscopy

Compound Me-2 (acylated methoxy-intermediate)

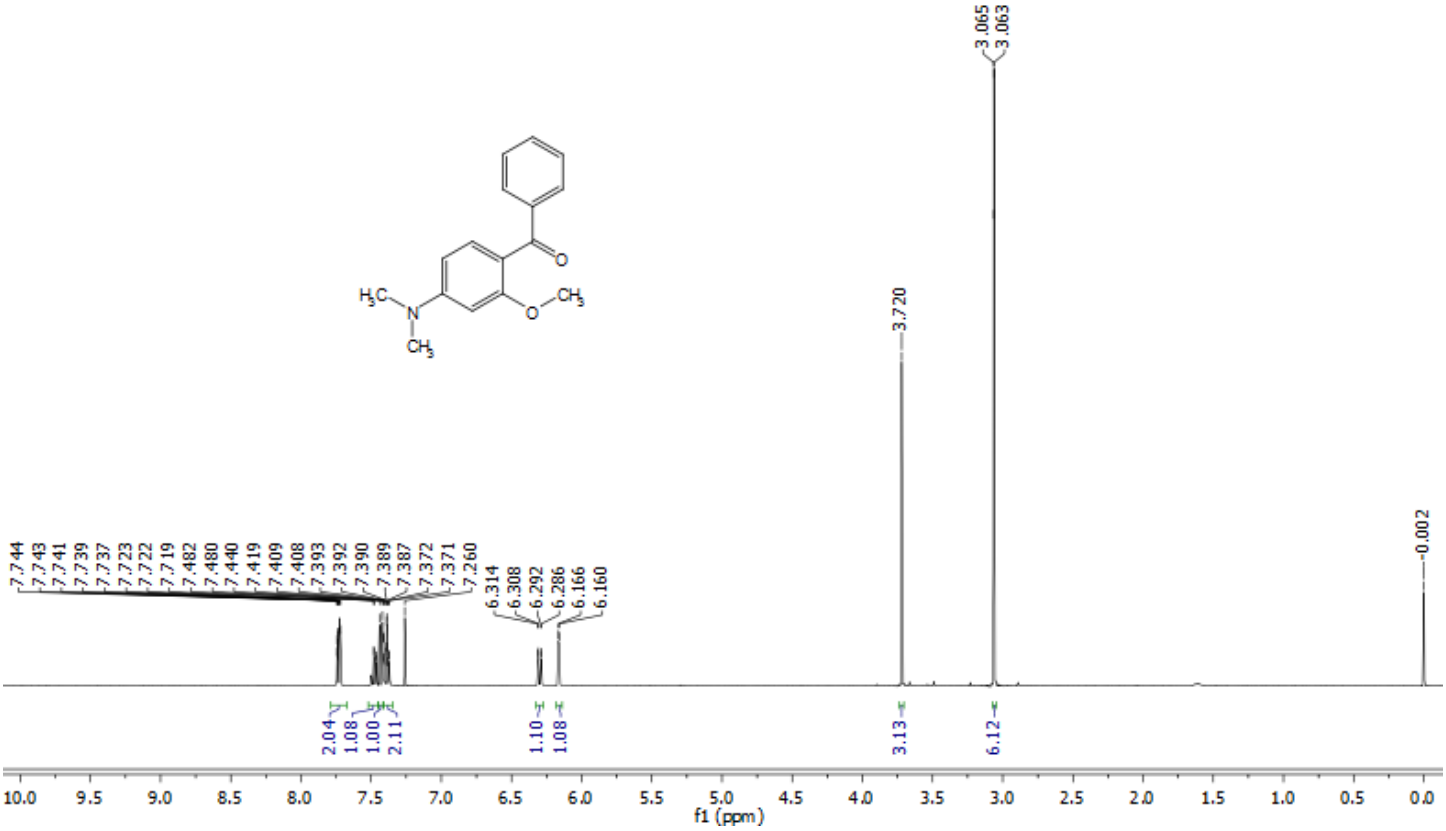

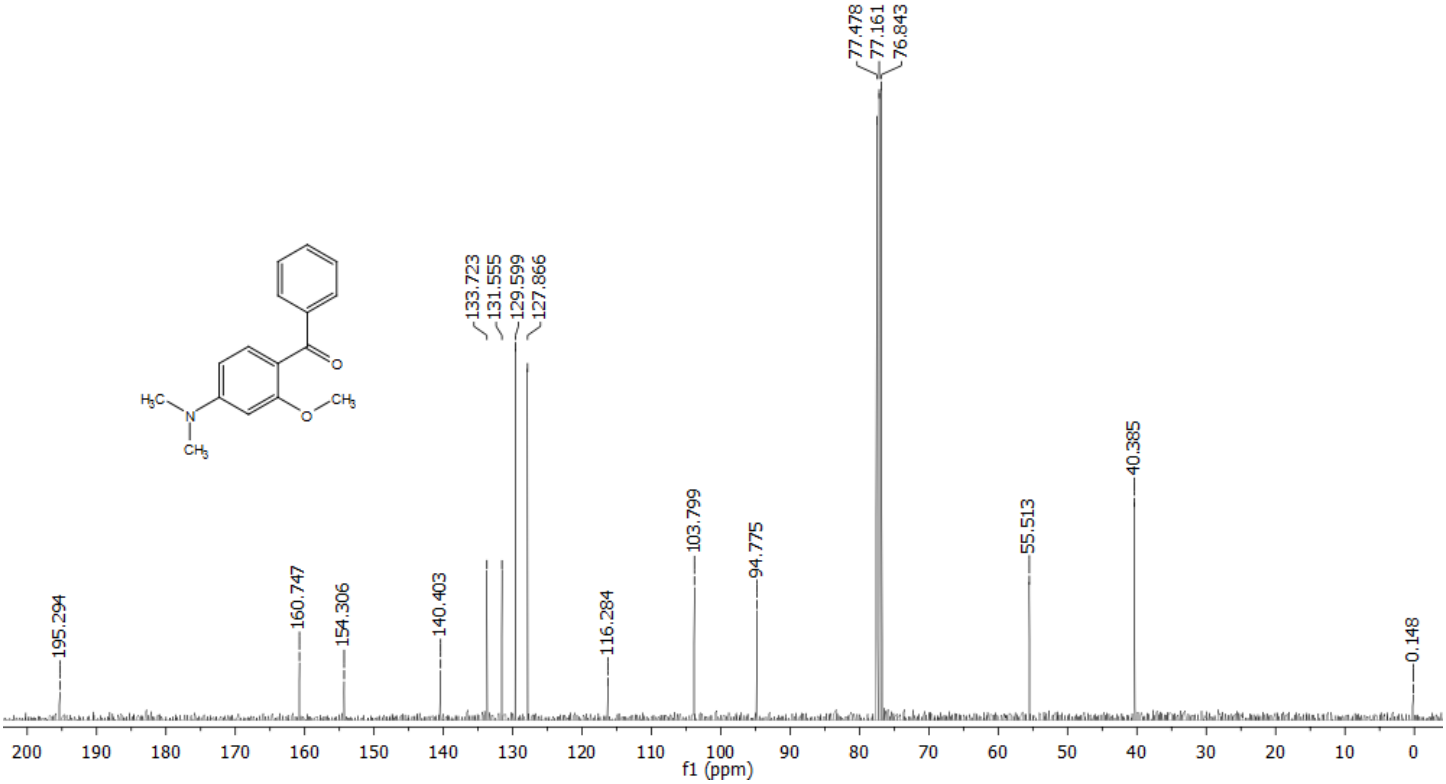

Compound Me-2

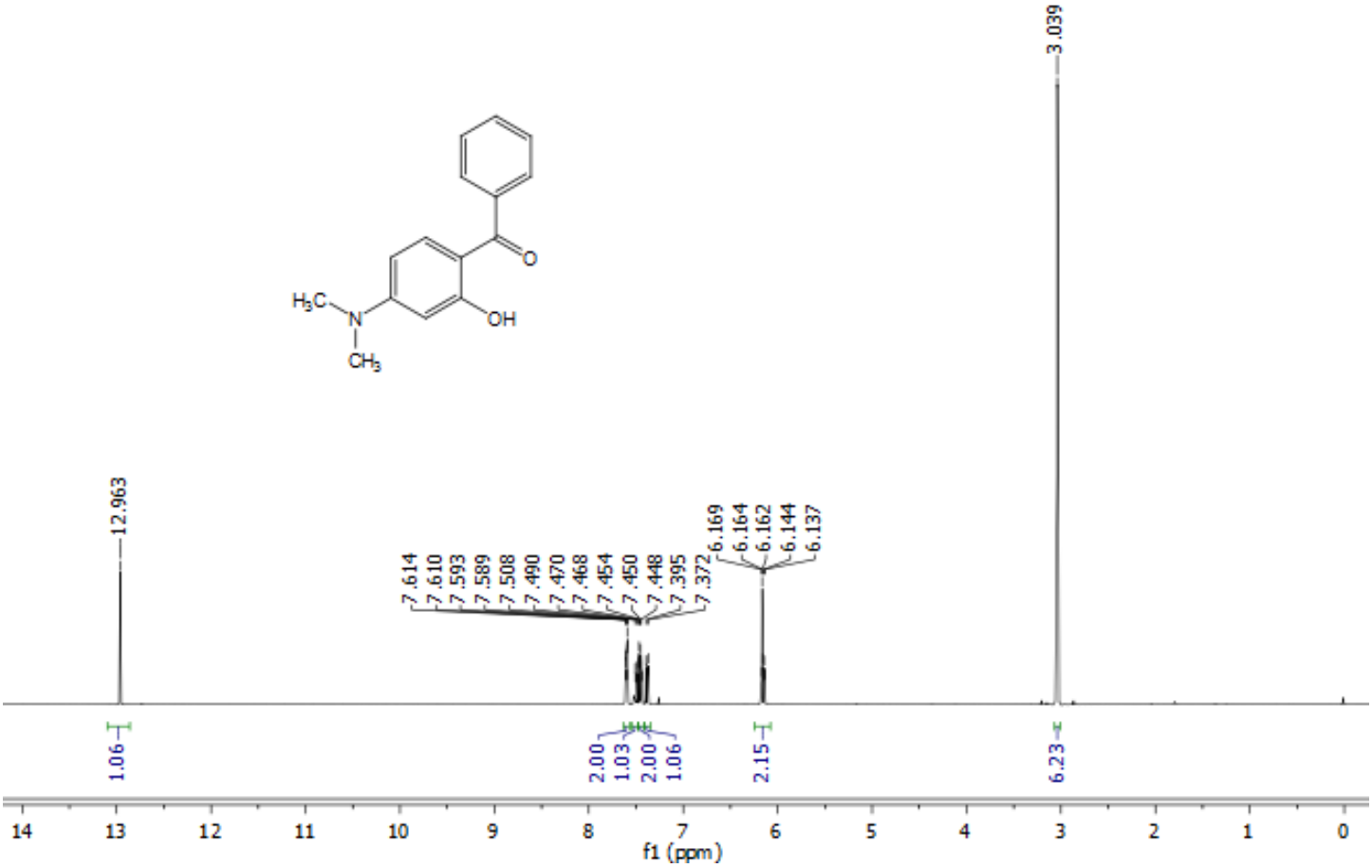

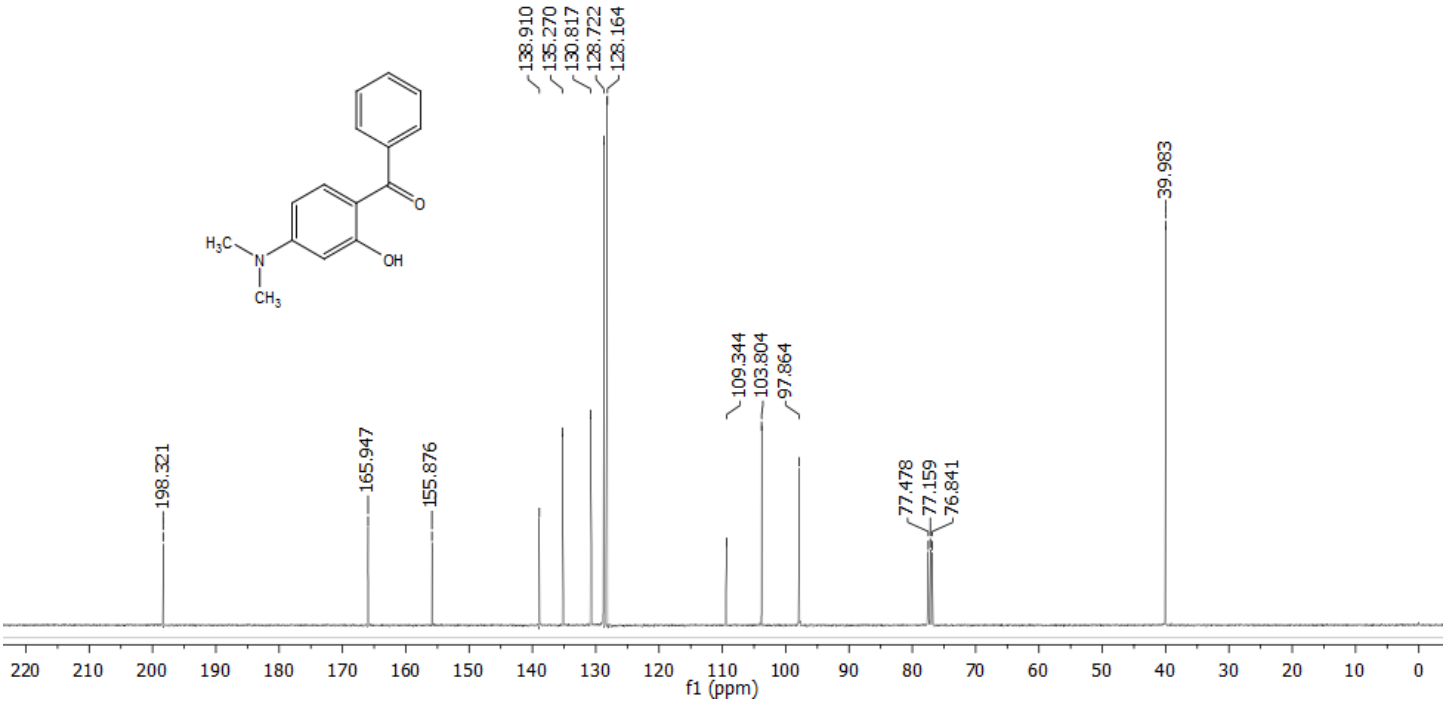

Me-Rosol

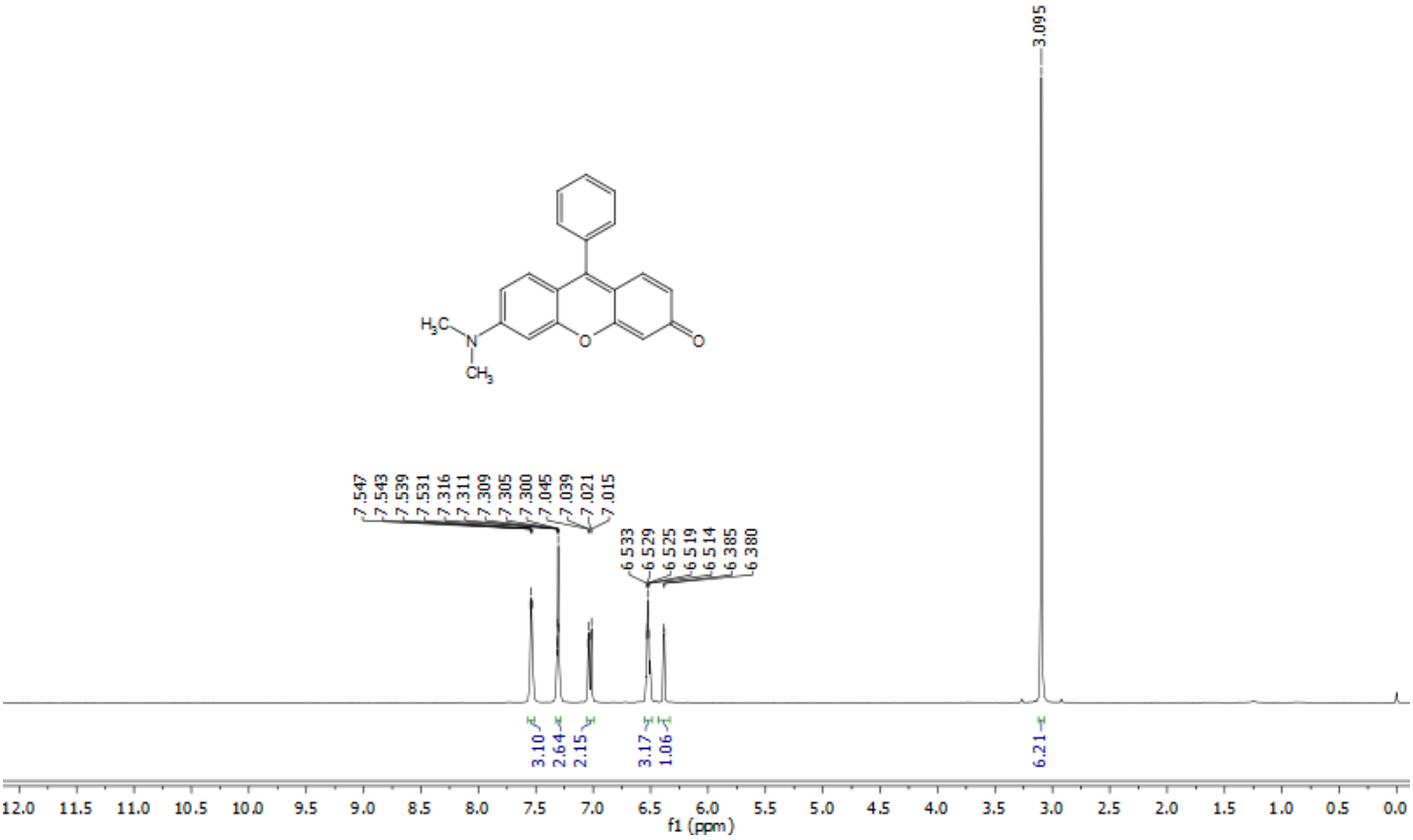
3.095
7.547
7.543
7.539
7.531
7.316
7.311
7.309
7.305
7.300
7.045
7.039
7.021
7.015
6.533
6.529
6.525
6.519
6.514
6.385
6.380
3.10
2.64
2.15
3.17
1.06
6.21
f1 (ppm)

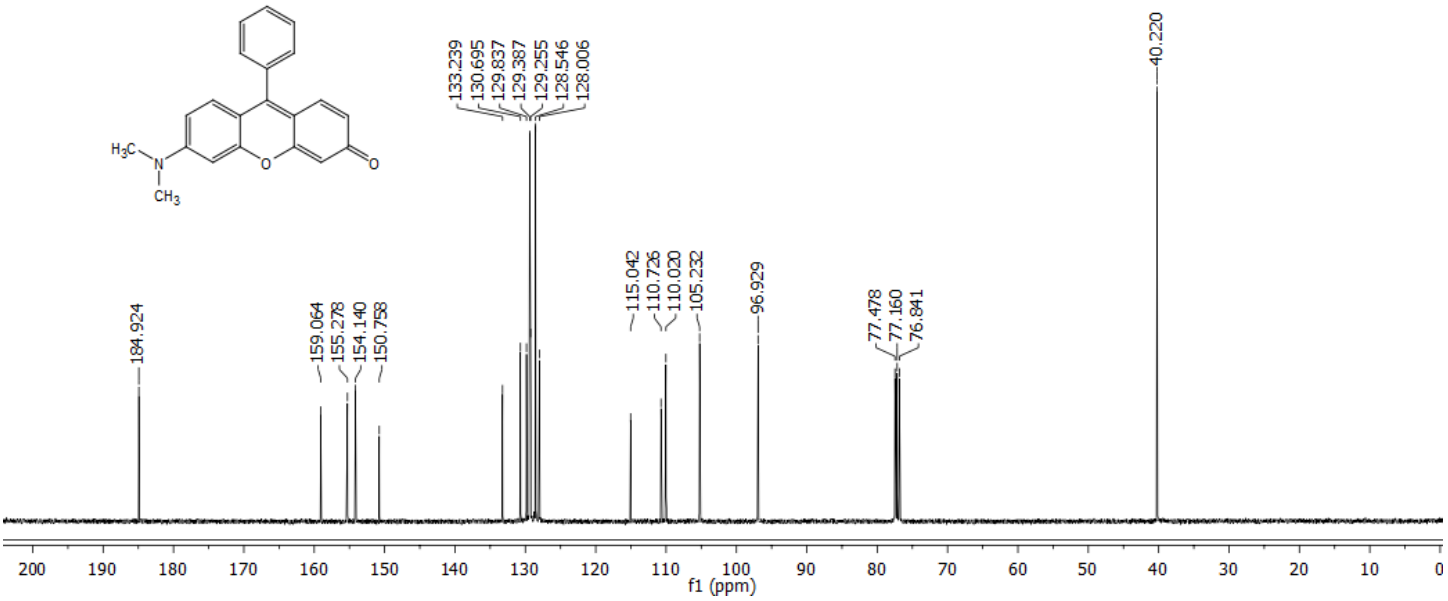
184.924
159.064
155.278
154.140
150.758
133.239
130.695
129.837
129.387
129.255
128.546
128.006
115.042
110.726
110.020
105.232
96.929
77.478
77.160
76.841
40.220
f1 (ppm)

Compound Et-2 (acylated methoxy-intermediate)

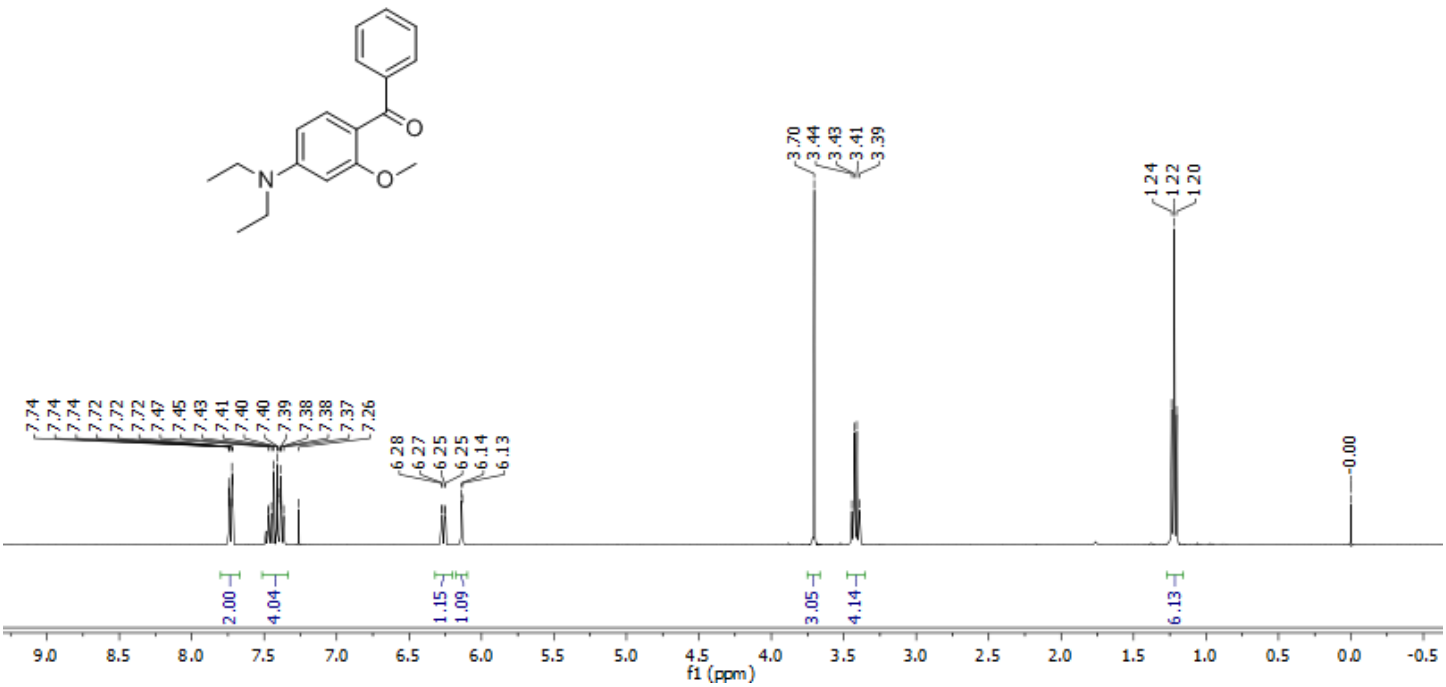

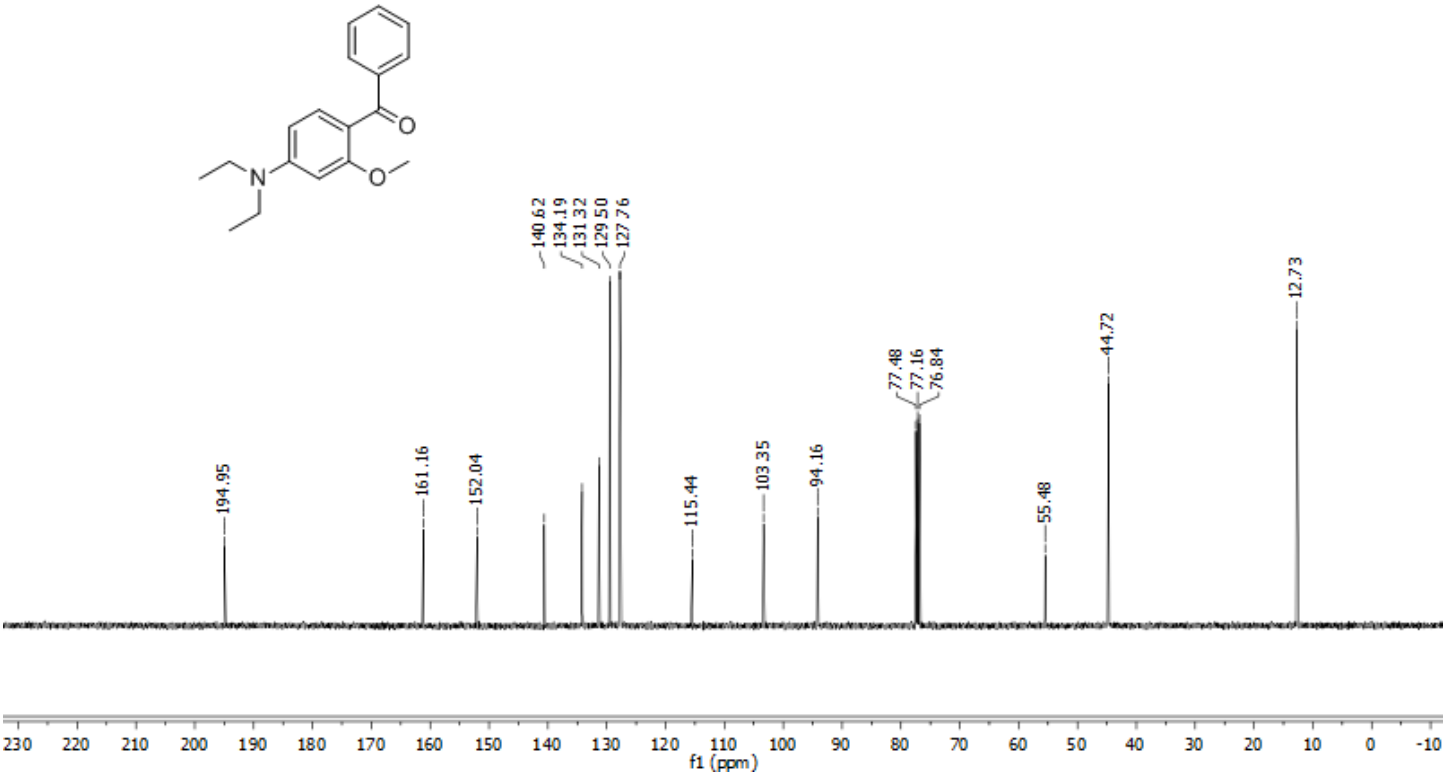

Compound Et-2

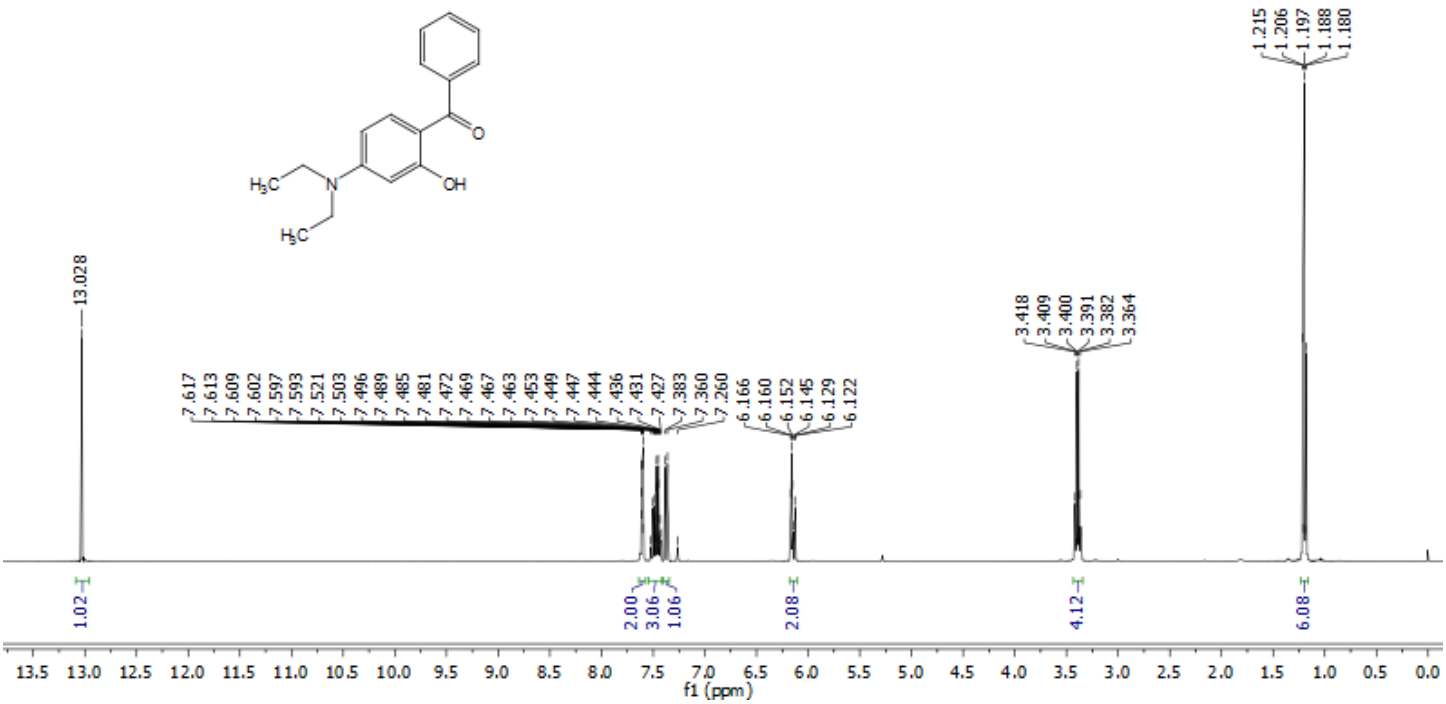

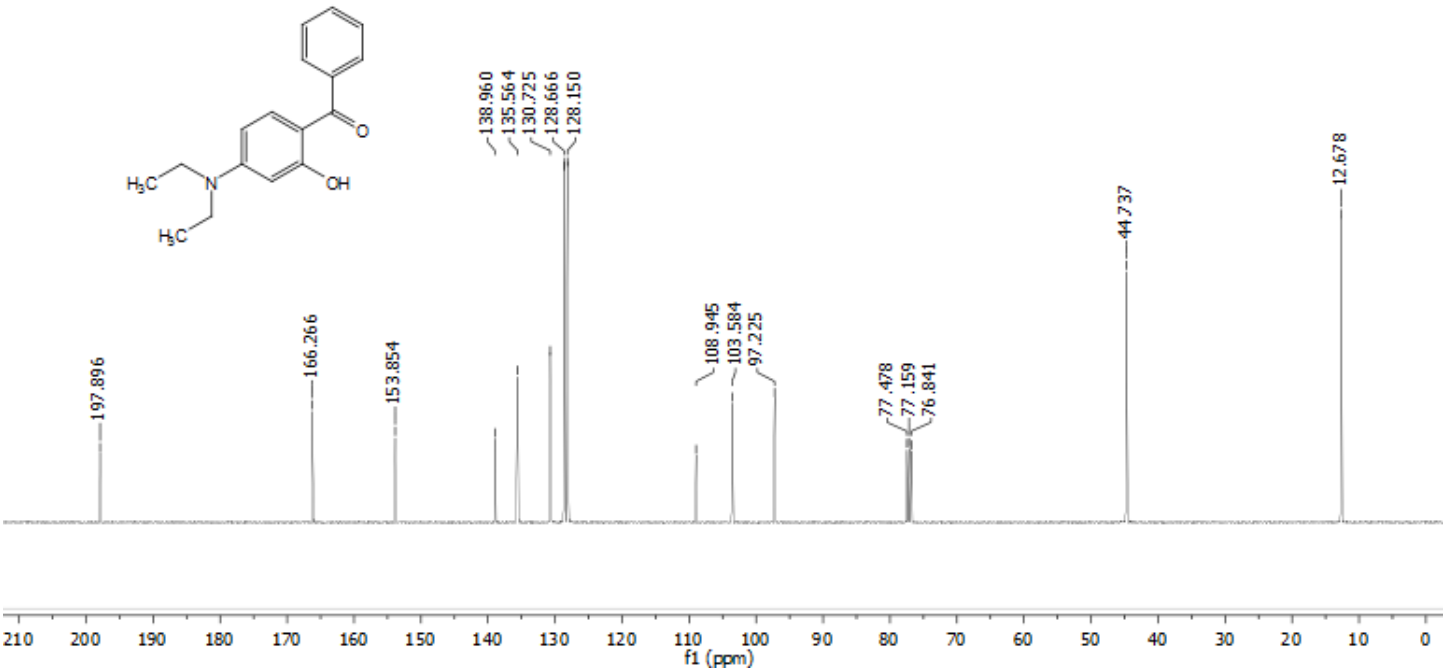

Et-Rosol

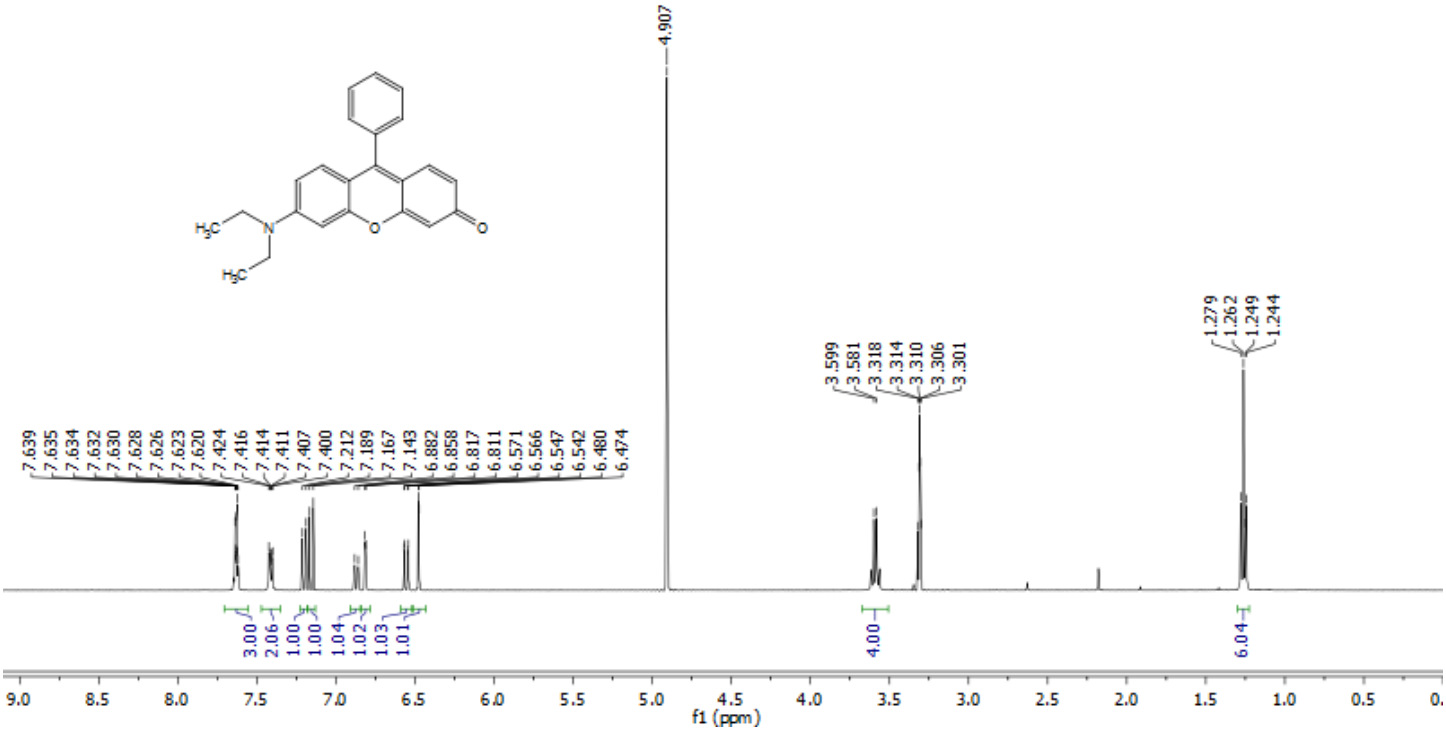
4.907
3.599
3.581
3.318
3.314
3.310
3.306
3.301
1.279
1.262
1.249
1.244
7.639
7.635
7.634
7.632
7.630
7.628
7.626
7.623
7.620
7.424
7.416
7.414
7.411
7.407
7.400
7.212
7.189
7.167
7.143
6.882
6.858
6.817
6.811
6.571
6.566
6.547
6.542
6.480
6.474
3.00
2.06
1.00
1.00
1.04
1.02
1.03
1.01
4.00
6.04
f1 (ppm)

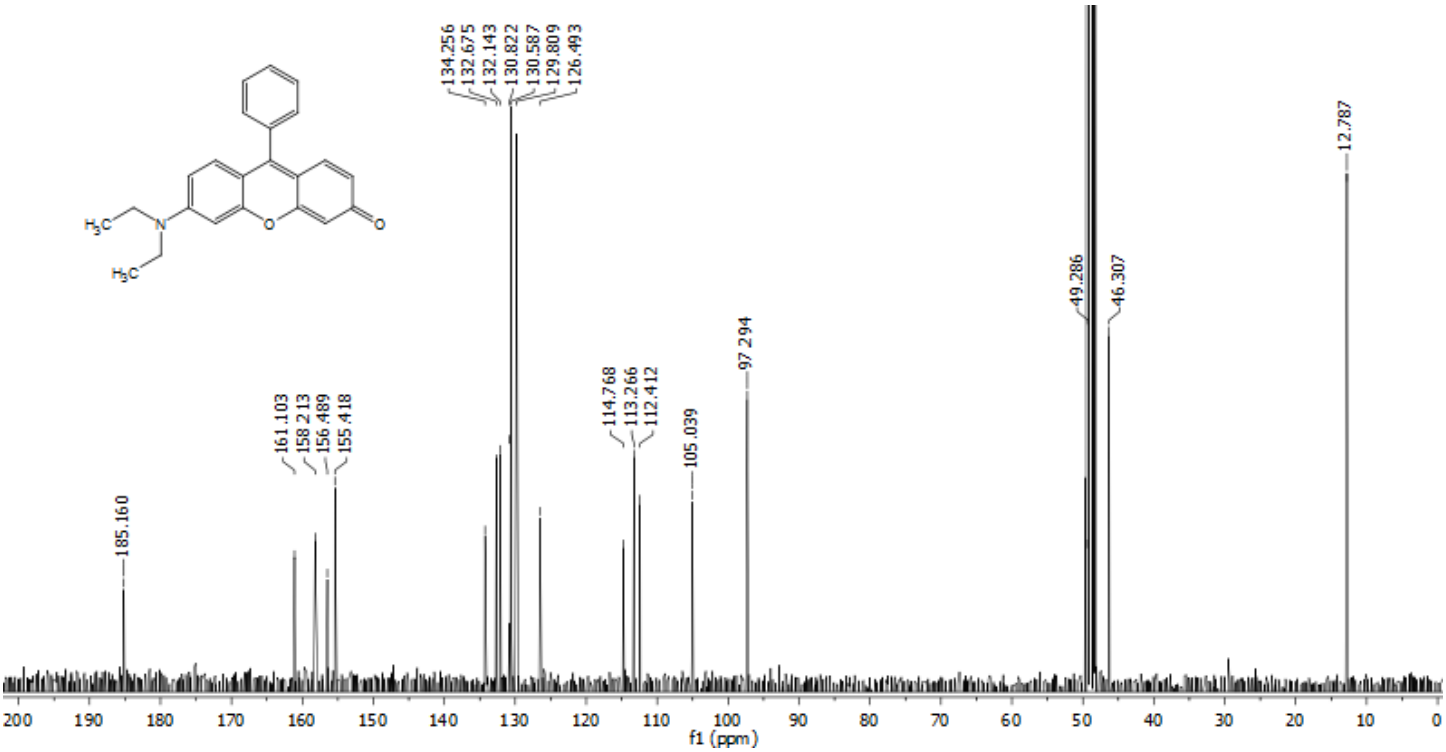
134.256
132.675
132.143
130.822
130.587
129.809
126.493
12.787
49.286
46.307
97.294
114.768
113.266
112.412
105.039
161.103
158.213
156.489
155.418
185.160
f1 (ppm)

Compound Pip-2 (acylated methoxy-intermediate)

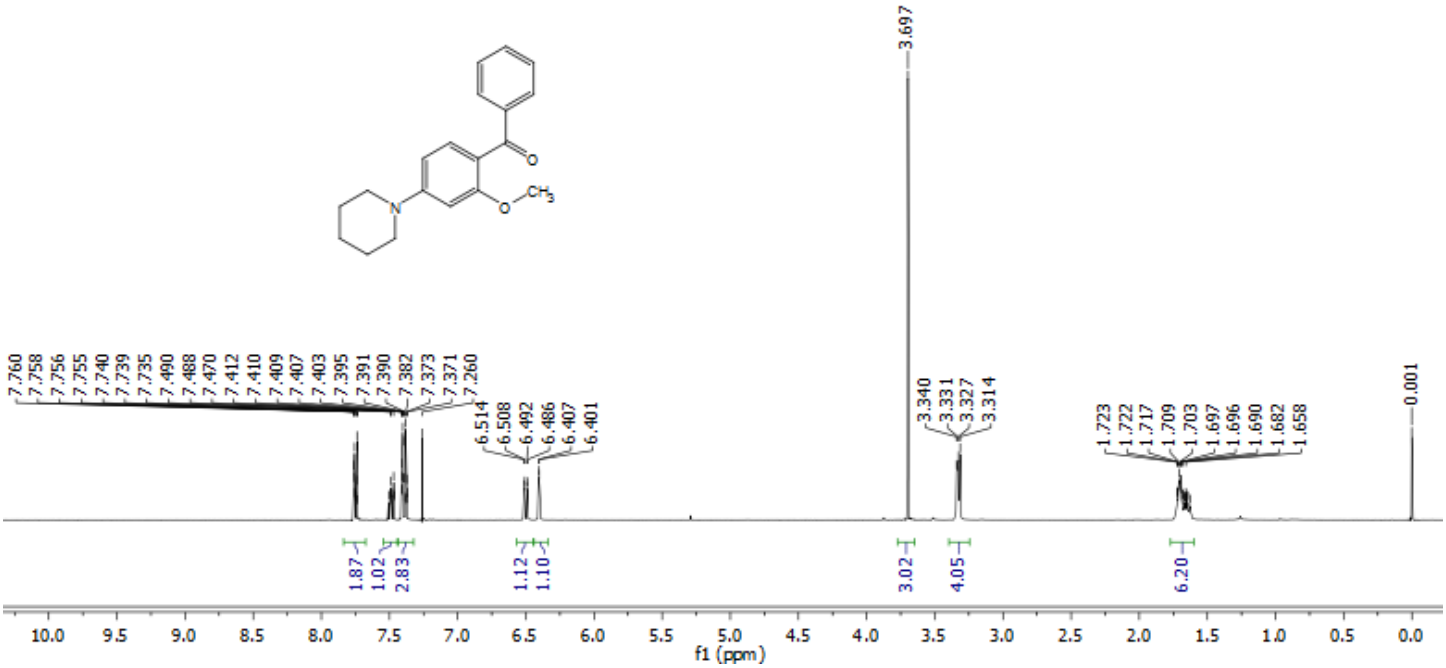

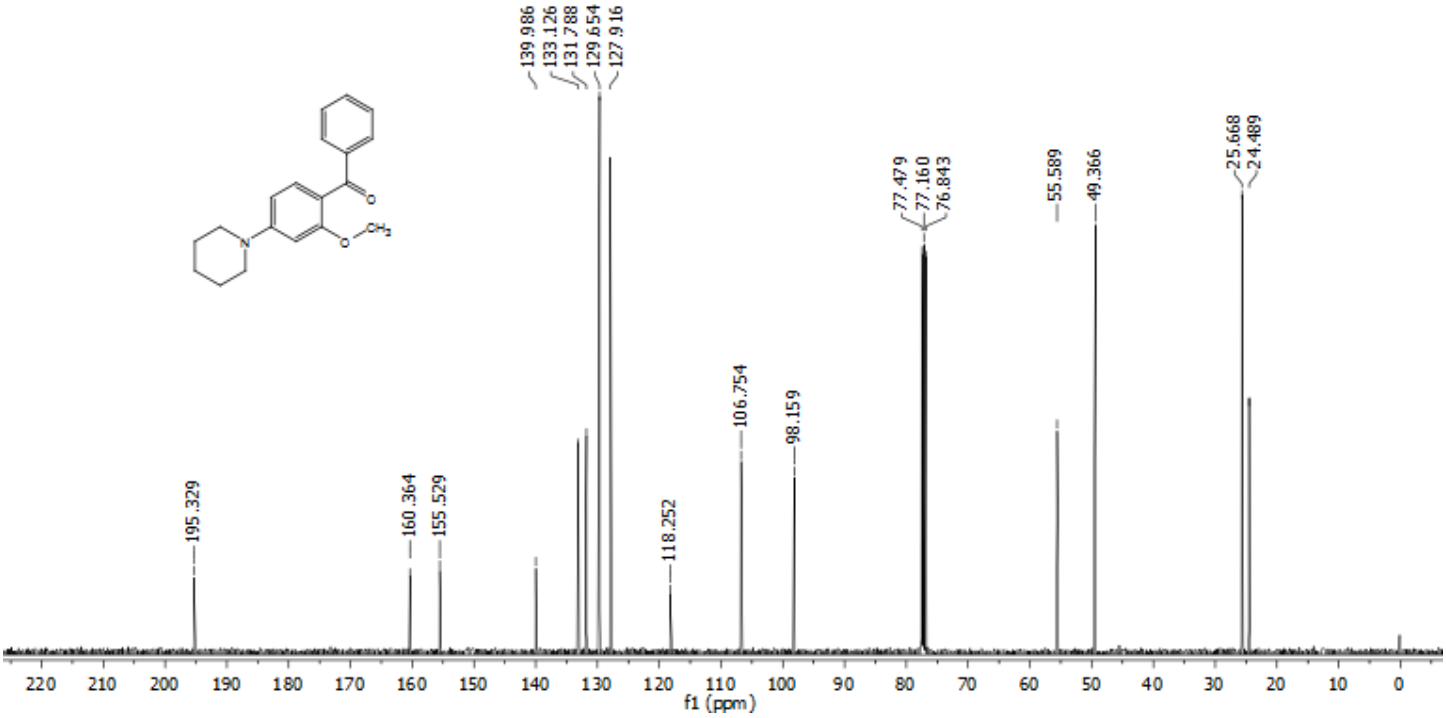

Compound Pip-2

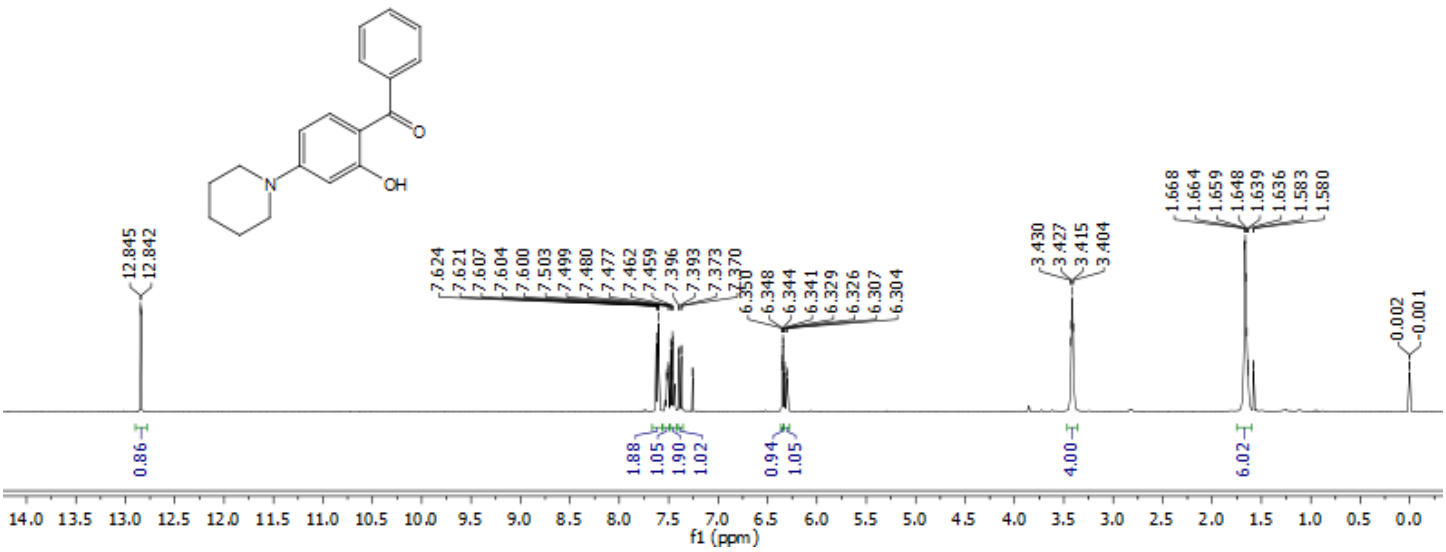

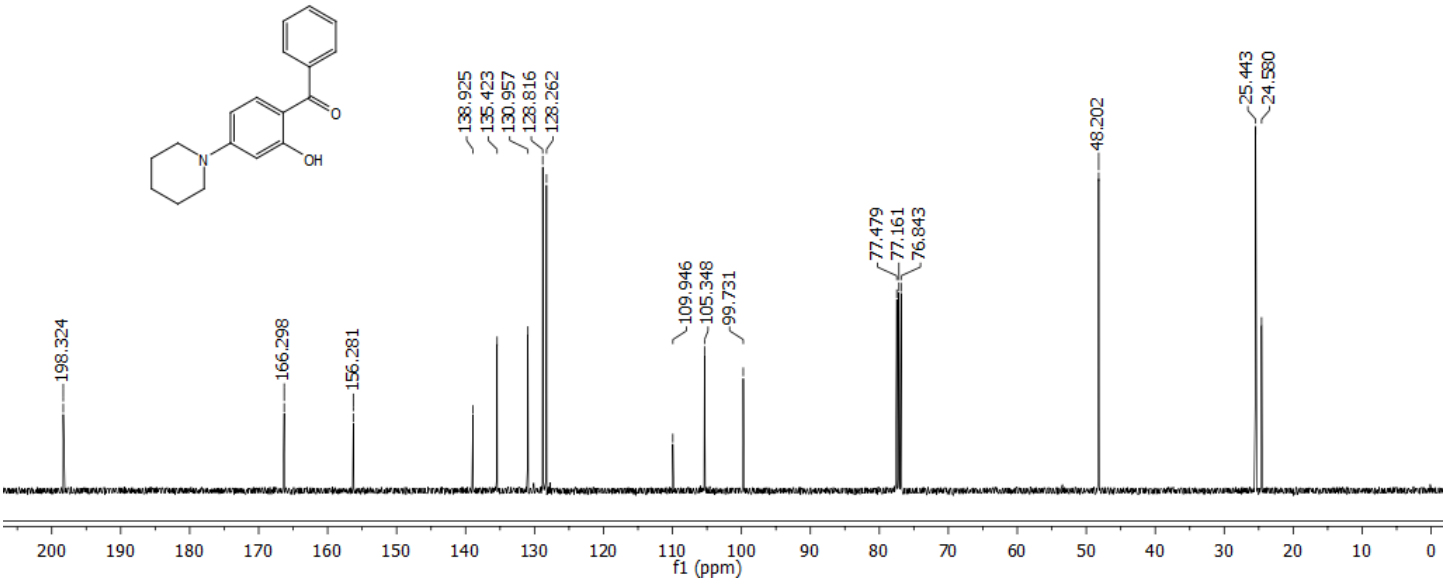

Pip-Rosol

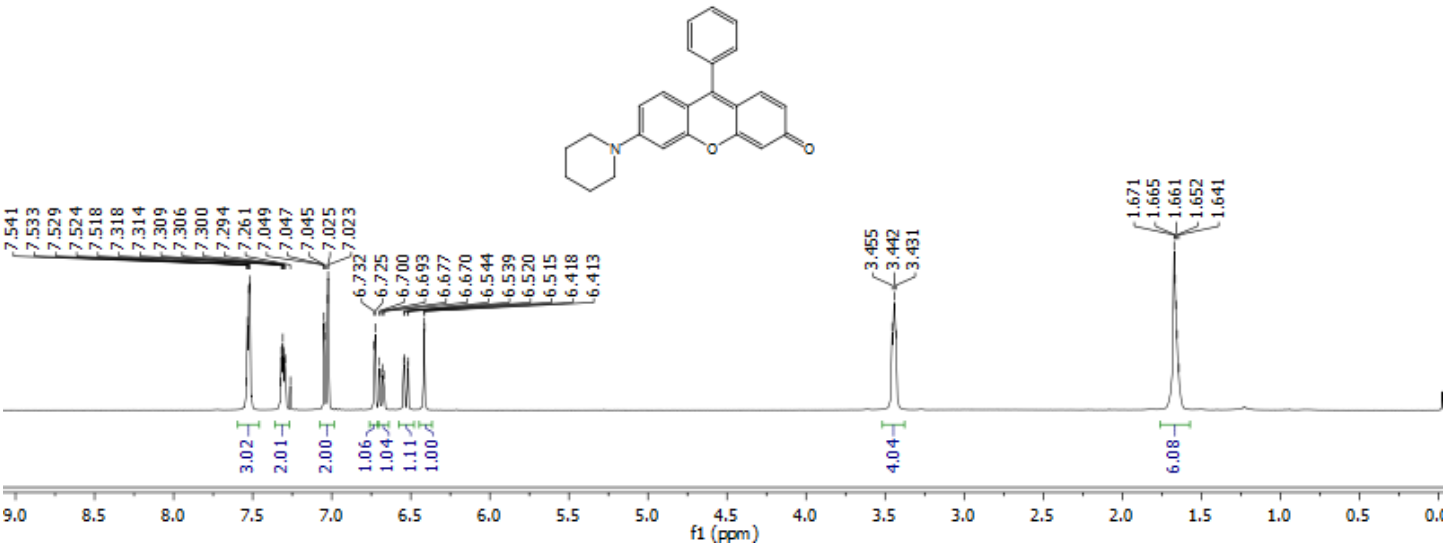
7.541
7.533
7.529
7.524
7.518
7.318
7.314
7.309
7.306
7.300
7.294
7.261
7.049
7.047
7.045
7.025
7.023
6.732
6.725
6.700
6.693
6.677
6.670
6.544
6.539
6.520
6.515
6.418
6.413
3.455
3.442
3.431
1.671
1.665
1.661
1.652
1.641
3.02
2.01
2.00
1.06
1.04
1.11
1.00
4.04
6.08
f1 (ppm)

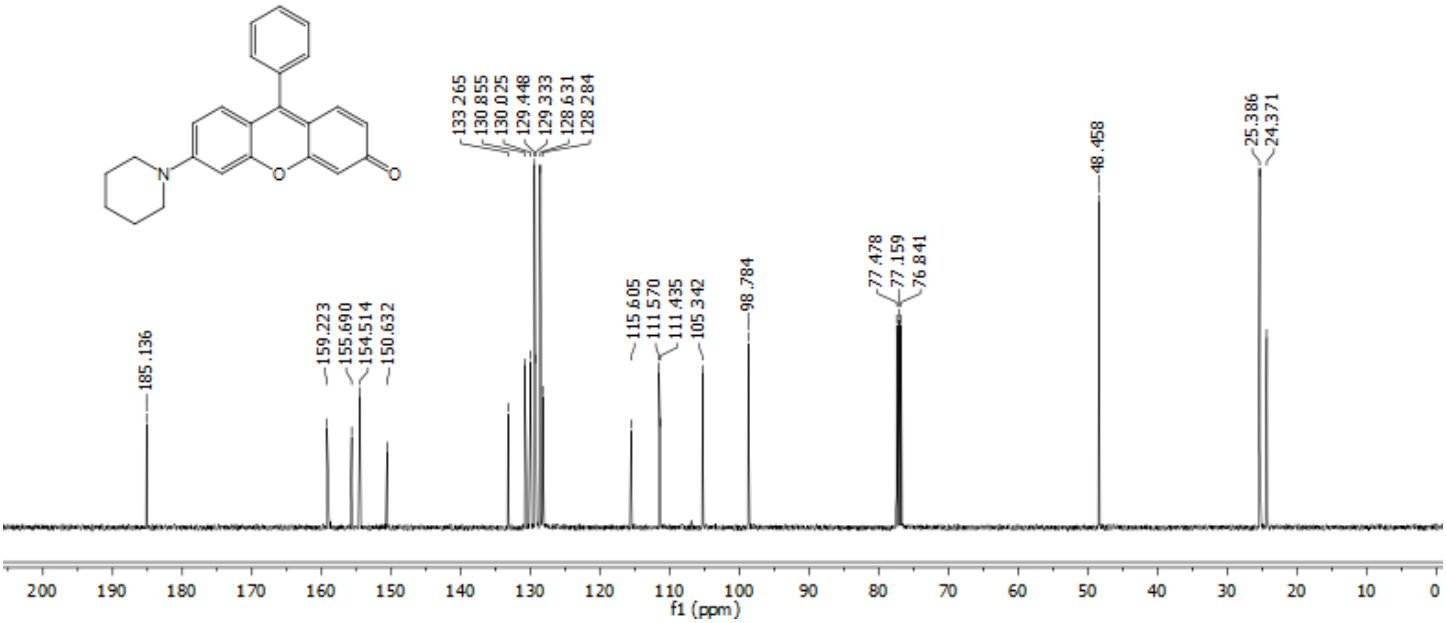
185.136
159.223
155.690
154.514
150.632
133.265
130.855
130.025
129.448
129.333
128.631
128.284
115.605
111.570
111.435
105.342
98.784
77.478
77.159
76.841
48.458
25.386
24.371
f1 (ppm)

Compound Jul-2 (acylated methoxy-intermediate)

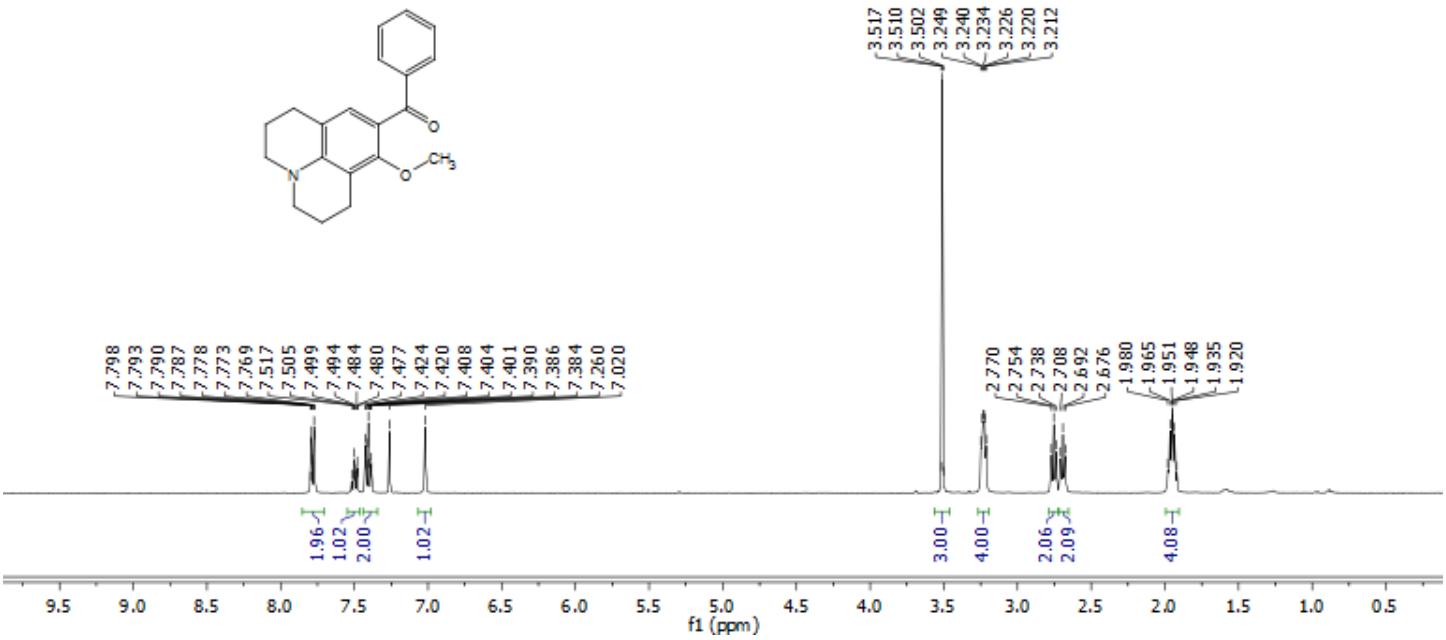

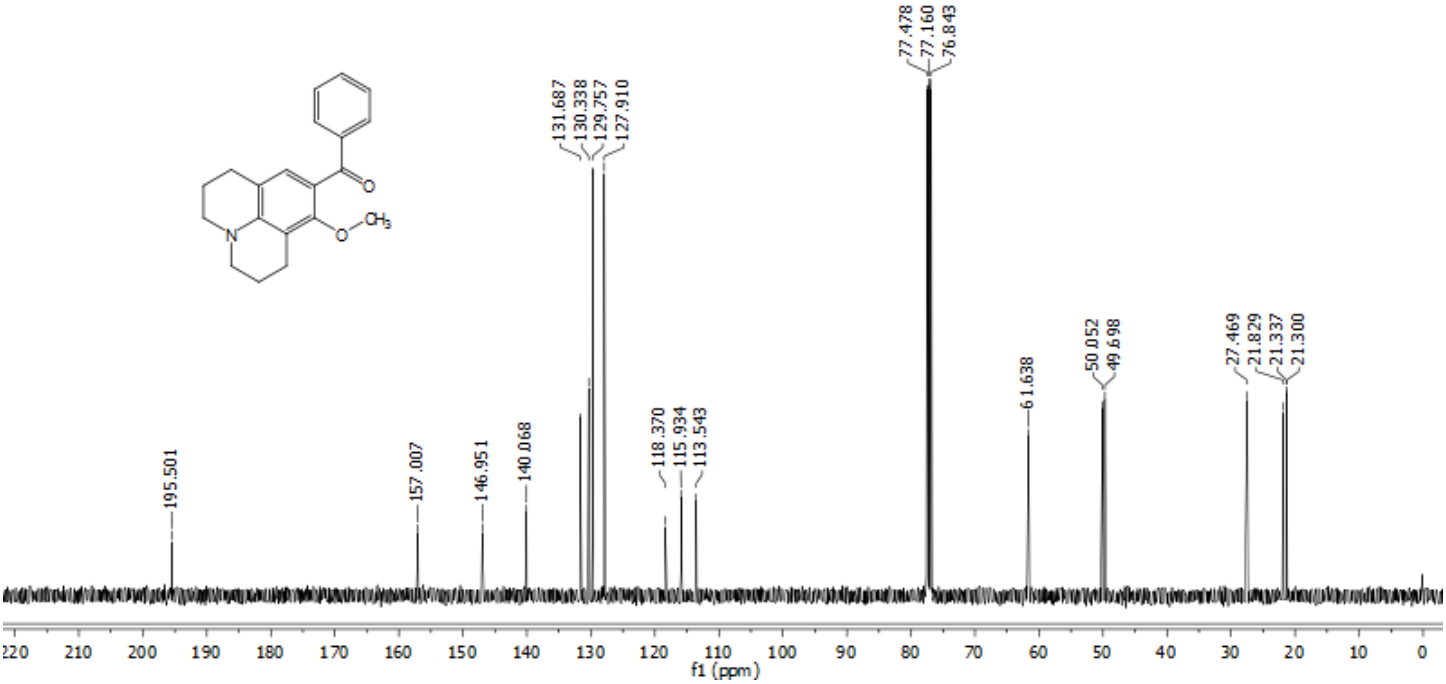

Compound Jul-2

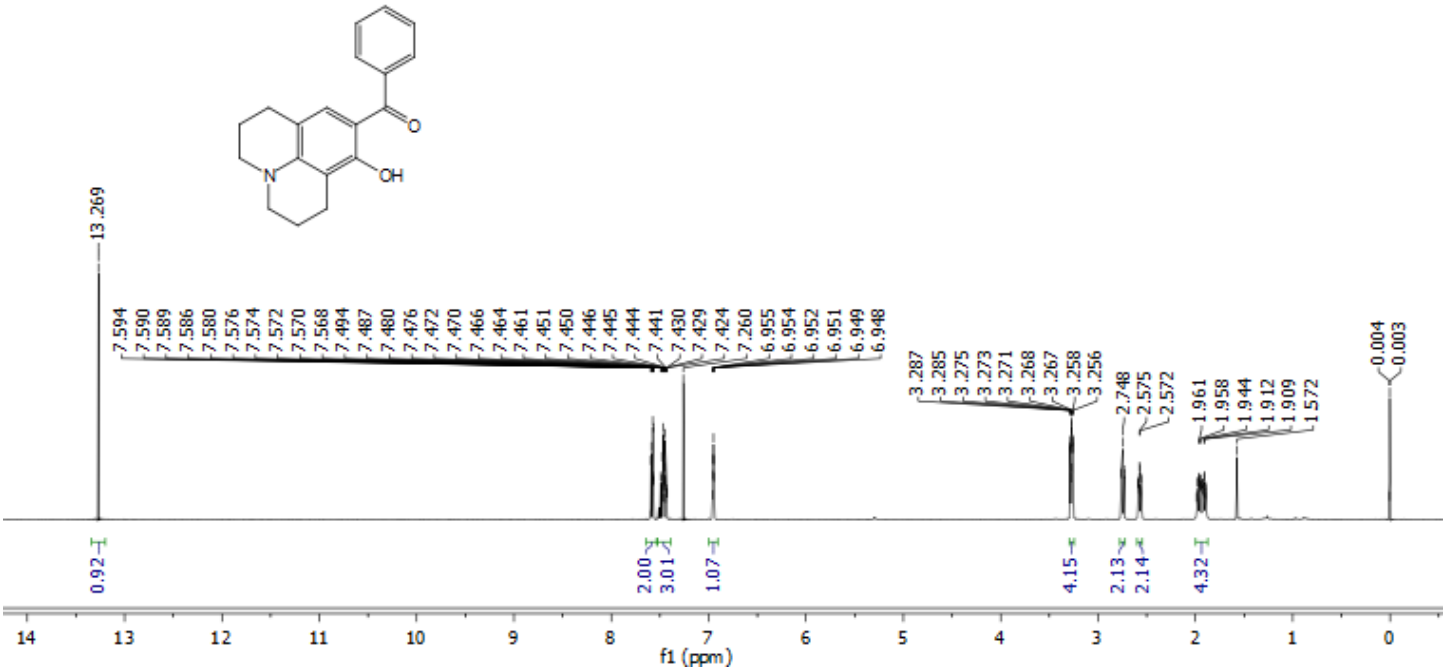

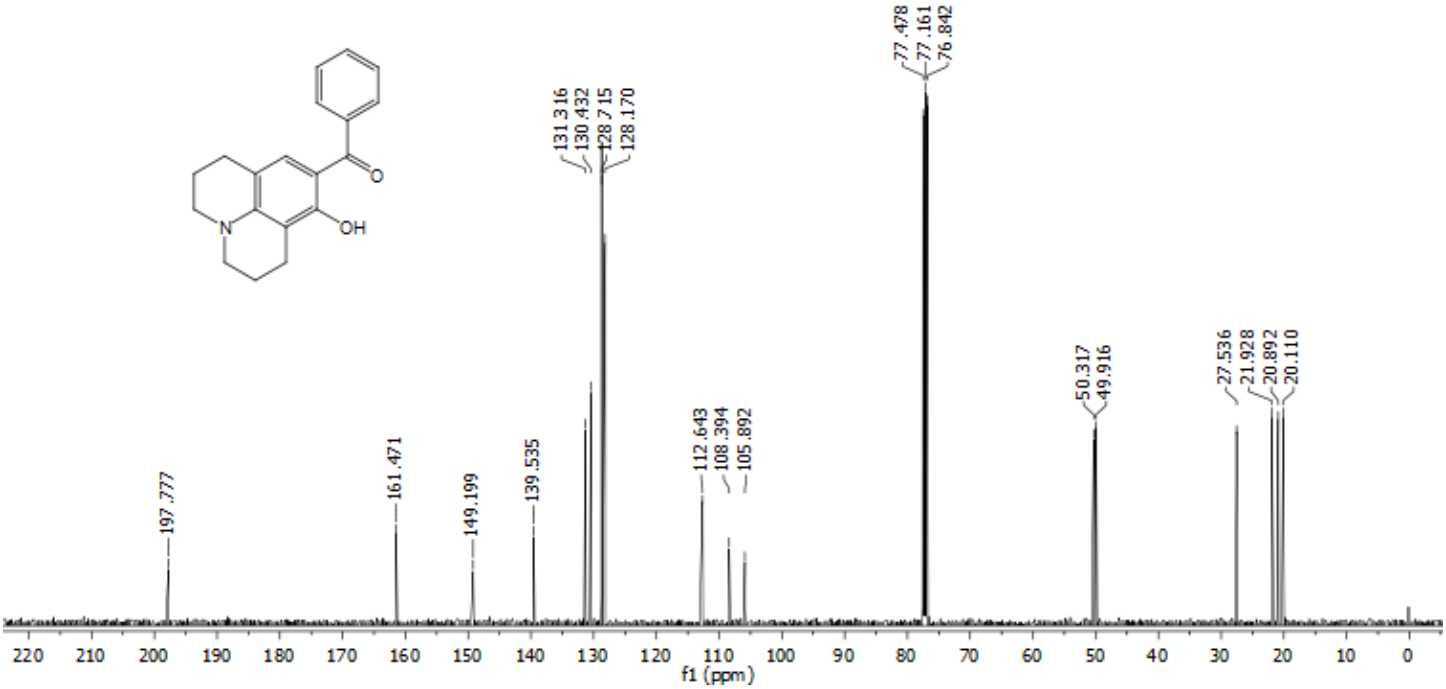

Jul-Rosol

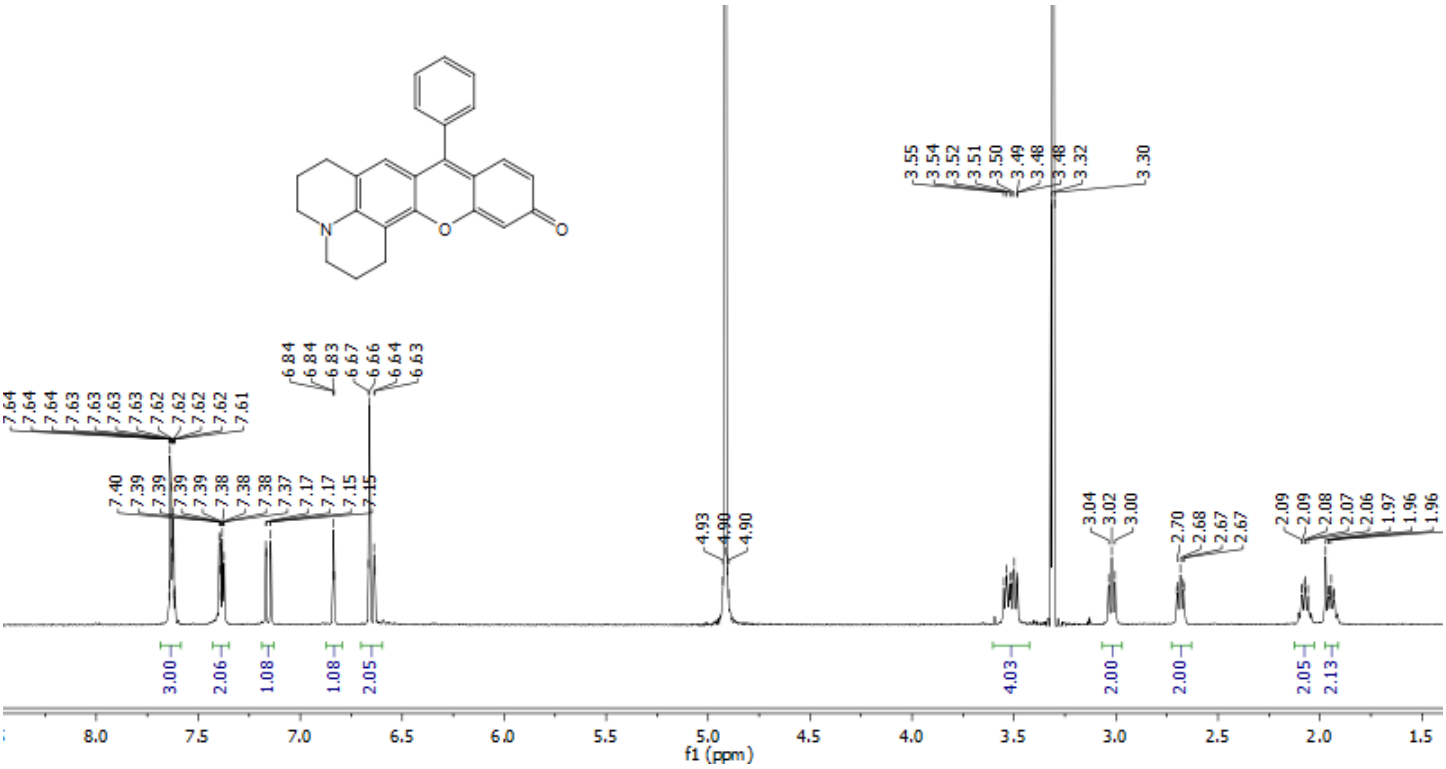
7.64
7.64
7.64
7.63
7.63
7.63
7.63
7.62
7.62
7.62
7.62
7.61
7.40
7.39
7.39
7.39
7.39
7.38
7.38
7.38
7.37
7.17
7.17
7.15
7.15
6.84
6.84
6.83
6.67
6.66
6.64
6.63
4.93
4.90
4.90
3.55
3.54
3.52
3.51
3.50
3.49
3.48
3.48
3.32
3.30
3.04
3.02
3.00
2.70
2.68
2.67
2.67
2.09
2.09
2.08
2.07
2.06
1.97
1.96
1.96
3.00
2.06
1.08
1.08
2.05
4.03
2.00
2.00
2.05
2.13
8.0
7.5
7.0
6.5
6.0
5.5
5.0
4.5
4.0
3.5
3.0
2.5
2.0
1.5
f1 (ppm)

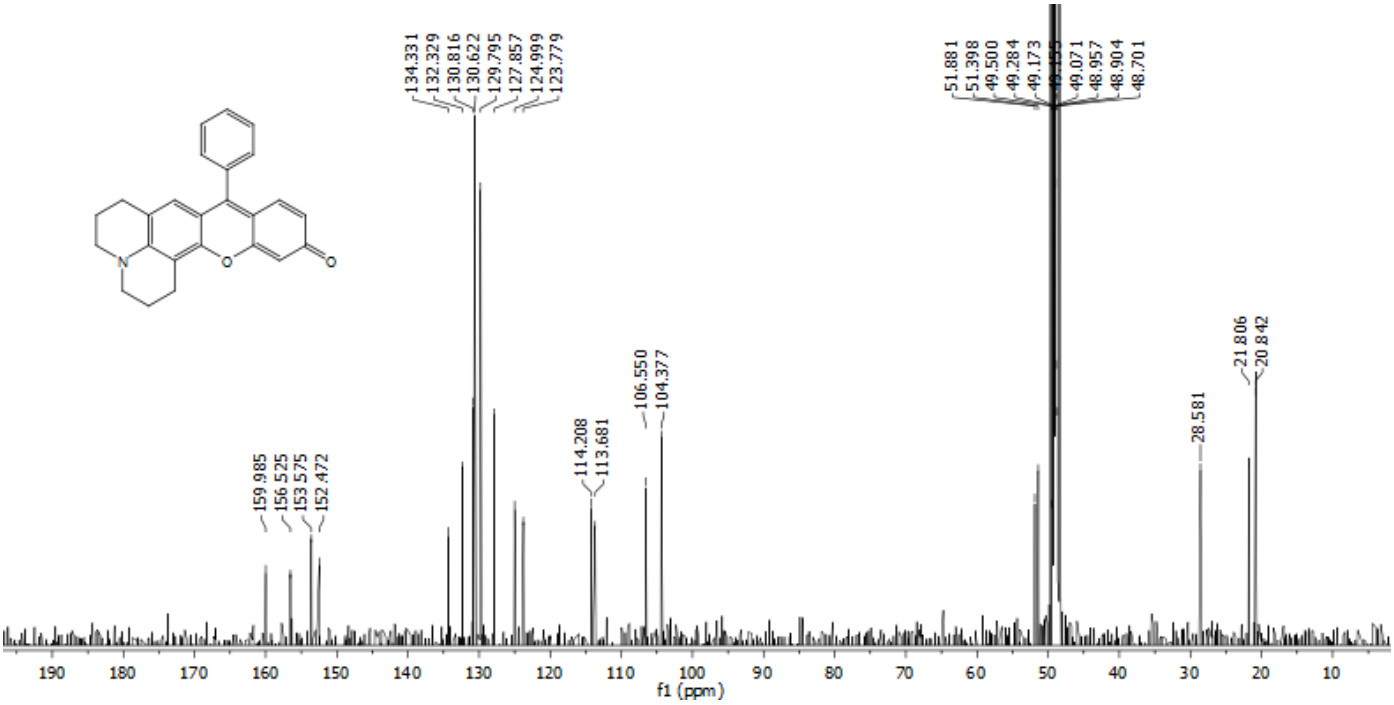
134.331
132.329
130.816
130.622
129.795
127.857
124.999
123.779
51.881
51.398
49.500
49.284
49.173
49.071
48.957
48.904
48.701
159.985
156.525
153.575
152.472
114.208
113.681
106.550
104.377
28.581
21.806
20.842
190
180
170
160
150
140
130
120
110
100
90
80
70
60
50
40
30
20
10
f1 (ppm)

Compound 4 (acylated methoxy-intermediate)

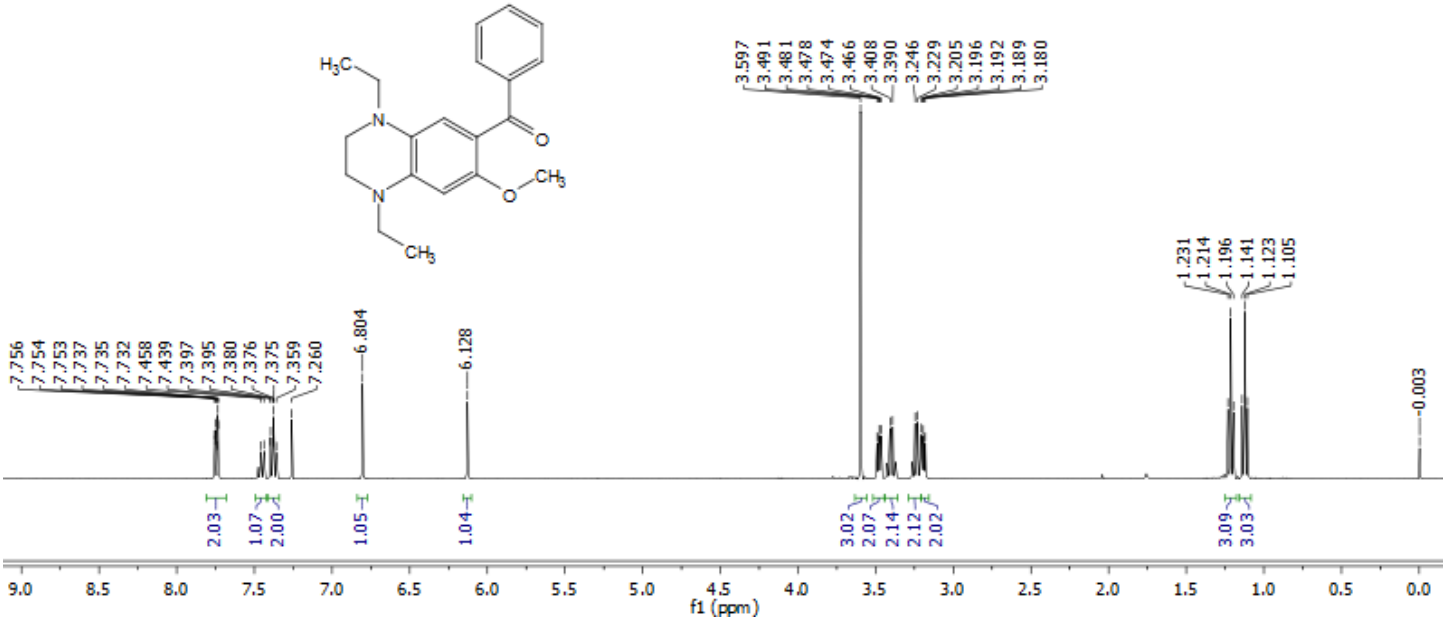

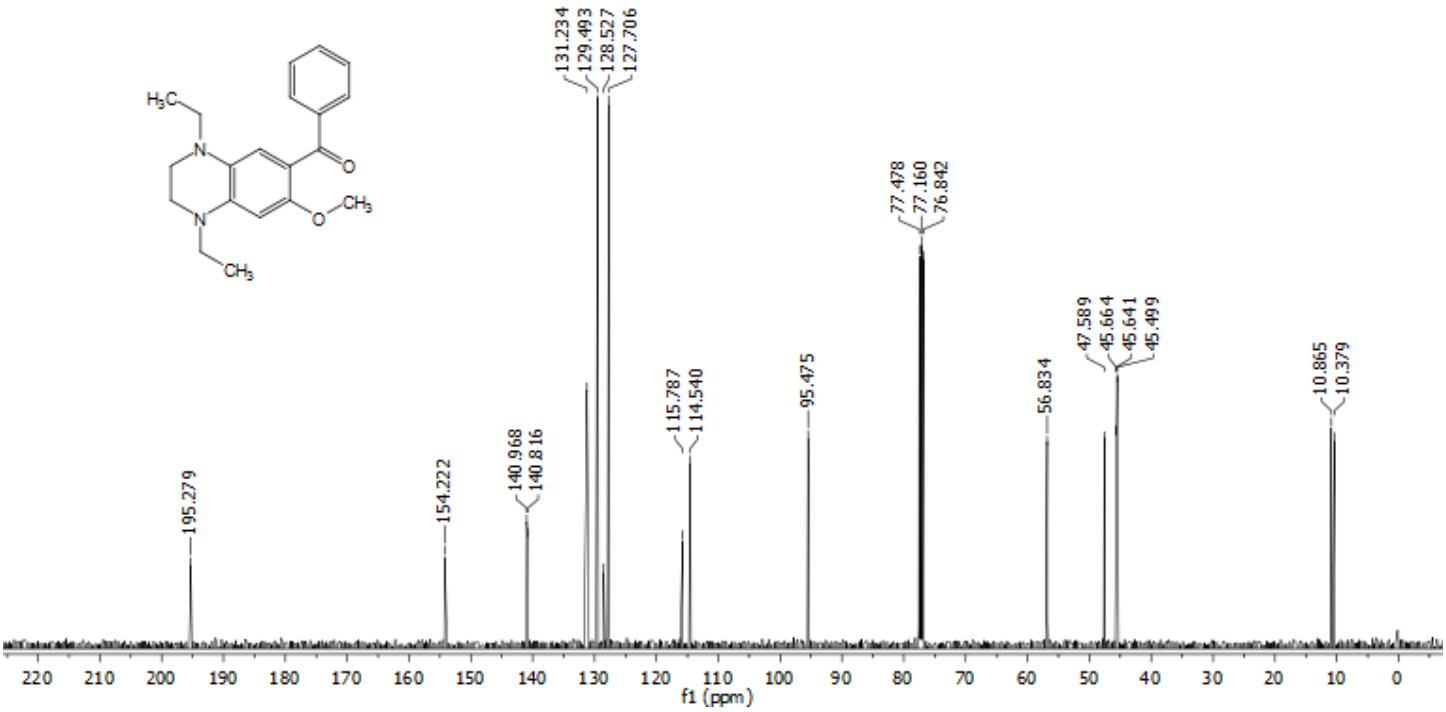

Compound 4

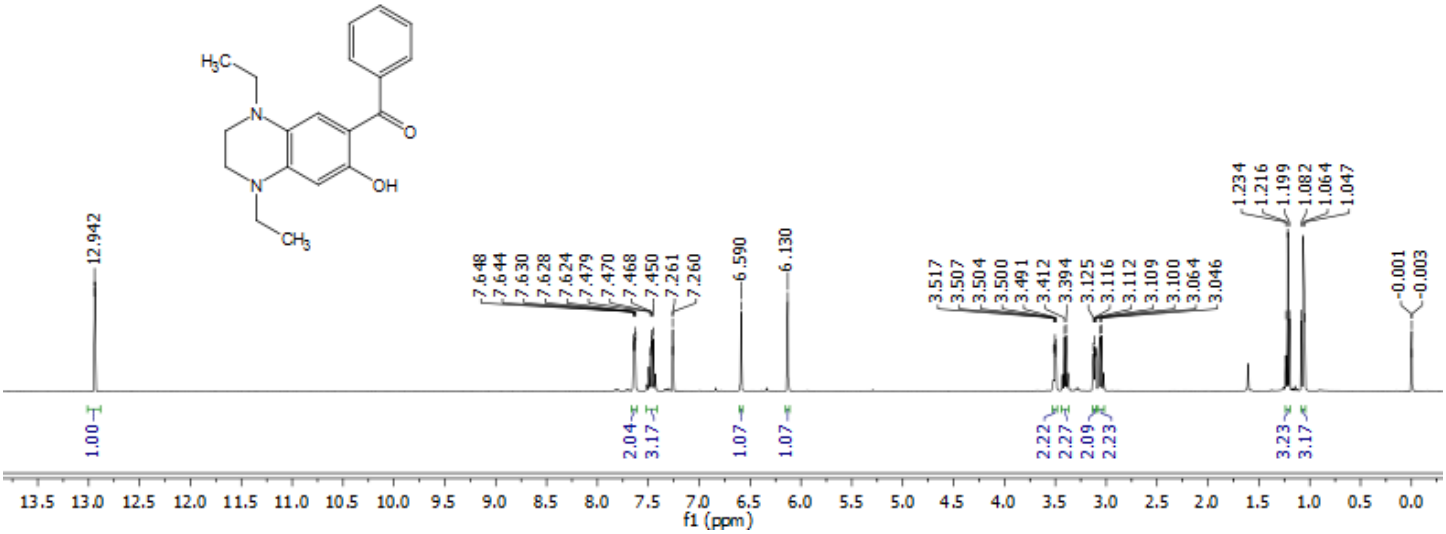
12.942
7.648
7.644
7.630
7.628
7.624
7.479
7.470
7.468
7.450
7.261
7.260
6.590
6.130
3.517
3.507
3.504
3.500
3.491
3.412
3.394
3.125
3.116
3.112
3.109
3.100
3.064
3.046
1.234
1.216
1.199
1.082
1.064
1.047
-0.001
-0.003
1.00
2.04
3.17
1.07
1.07
2.22
2.27
2.09
2.23
3.23
3.17
f1 (ppm)

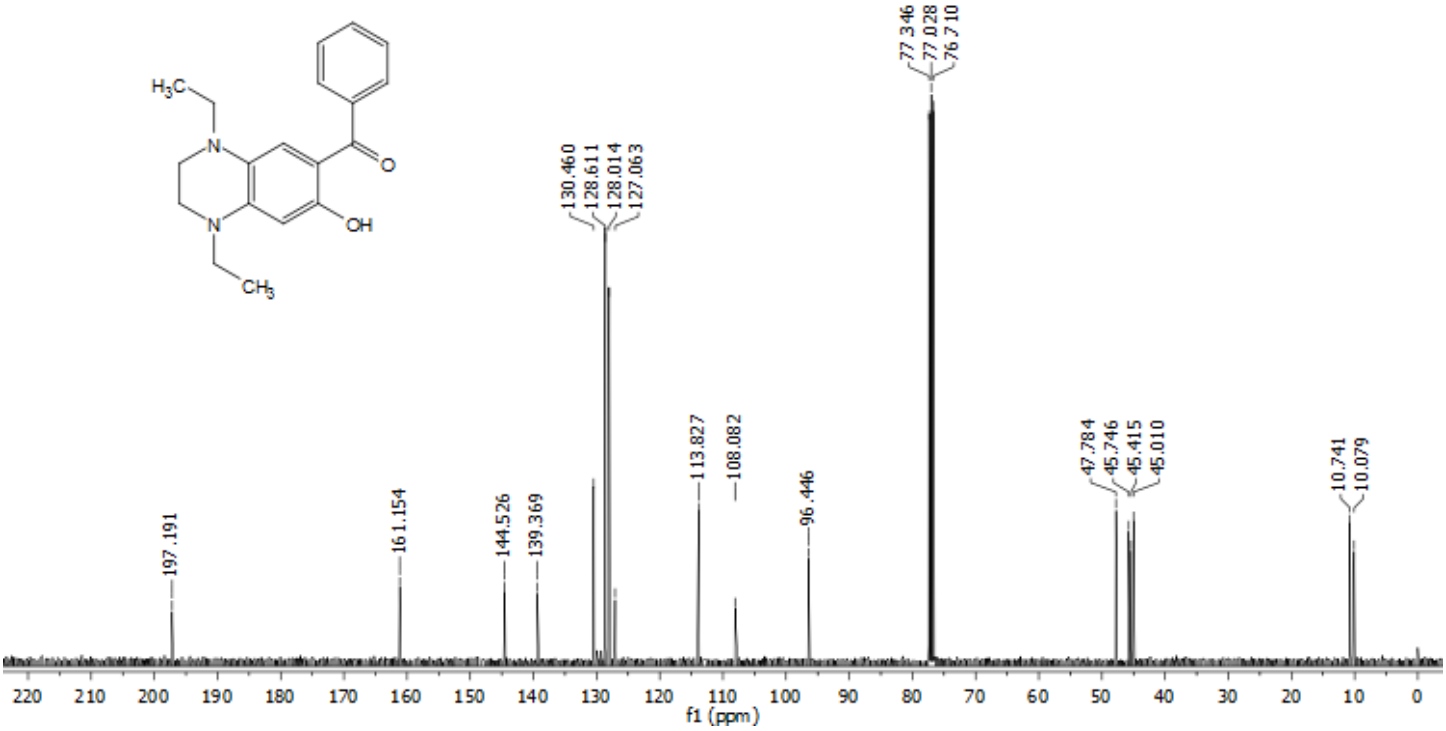
197.191
161.154
144.526
139.369
130.460
128.611
128.014
127.063
113.827
108.082
96.446
77.346
77.028
76.710
47.784
45.746
45.415
45.010
10.741
10.079
f1 (ppm)

THQ-Rosol

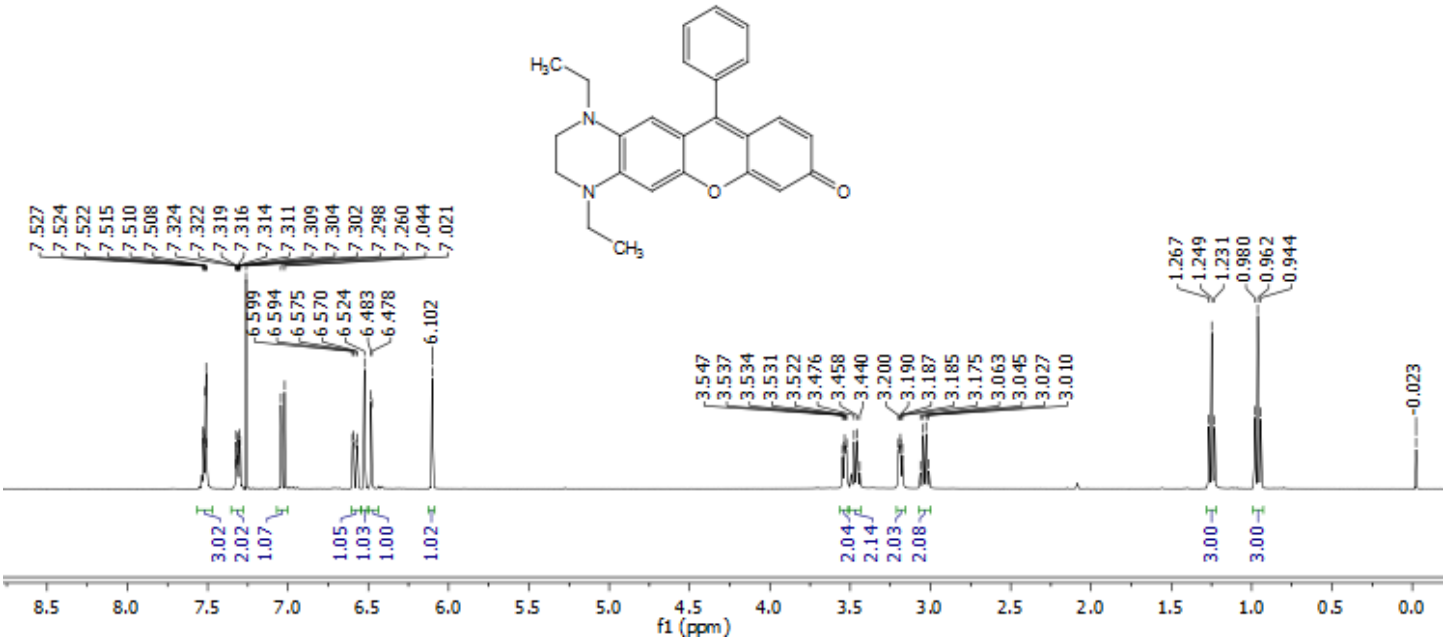
7.527
7.524
7.522
7.515
7.510
7.508
7.324
7.322
7.319
7.316
7.314
7.311
7.309
7.304
7.302
7.298
7.260
7.044
7.021
6.599
6.594
6.575
6.570
6.524
6.483
6.478
6.102
3.547
3.537
3.534
3.531
3.522
3.476
3.458
3.440
3.200
3.190
3.187
3.185
3.175
3.063
3.045
3.027
3.010
1.267
1.249
1.231
0.980
0.962
0.944
-0.023
3.02
2.02
1.07
1.05
1.03
1.00
1.02
2.04
2.14
2.03
2.08
3.00
3.00
8.5
8.0
7.5
7.0
6.5
6.0
5.5
5.0
4.5
4.0
3.5
3.0
2.5
2.0
1.5
1.0
0.5
0.0
f1 (ppm)

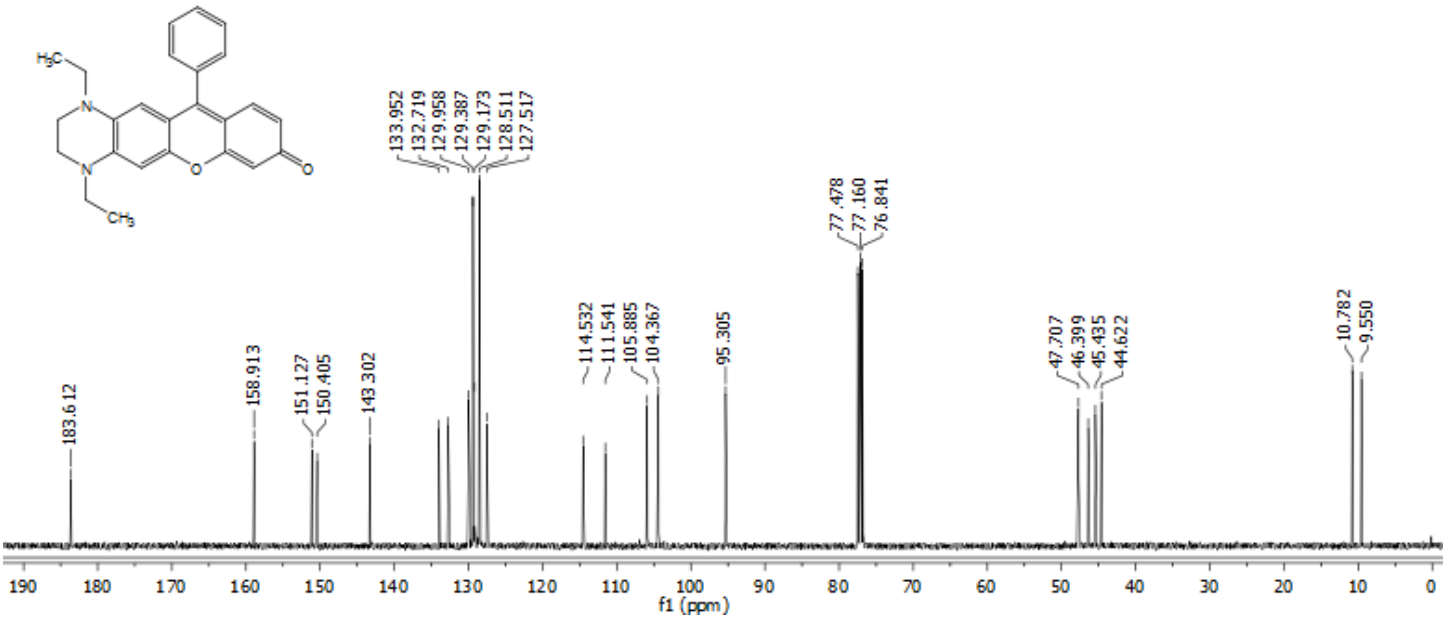
133.952
132.719
129.958
129.387
129.173
128.511
127.517
77.478
77.160
76.841
114.532
111.541
105.885
104.367
95.305
47.707
46.399
45.435
44.622
10.782
9.550
183.612
158.913
151.127
150.405
143.302
190
180
170
160
150
140
130
120
110
100
90
80
70
60
50
40
30
20
10
0
f1 (ppm)

8. References

1. Gaigalas, A. K. and Wang, L. Measurement of the Fluorescence Quantum Yield Using a Spectrometer with an Integrating Sphere Detector. *J. Res. Natl. Inst. Stand. Technol.* **2008**, *113*, 17-28.

2. Lakowicz, J. R. *Principles of Fluorescence Spectroscopy*, 3rd ed.; Springer: New York, 2006.

3. Vazquez, M. E.; Blanco, J. B.; Imperiali, B. Photophysics and Biological Applications of the Environment-Sensitive Fluorophore 6-*N,N*-Dimethylamino-2,3-naphthalimide. *J. Am. Chem. Soc.* **2005**, *127*, 1300-1306.

4. Gao, S.; Hao, L.; Li, J.; Lin, P.; Li, D.; Shuang, S.; Dong, C. Photophysical processes of an intramolecular charge transfer fluorescent dye with carbazole units. *Luminescence* **2013**, *28*, 412-418.

5. Loukova, G. V.; Vasiliev, V. P.; Milov, A. A.; Smirnov, V. A.; Minkin, V. I. Unraveling electronic properties of an organometallic solute: Lippert-Mataga and quantum-chemical extensive study. *J. Photochem. Photobiol. A* **2016**, *327*, 6-14.

6. Mishra, A.; Sahu, S.; Tripathi, S.; Krishnamoorthy, G. Photoinduced intramolecular charge transfer in *trans*-2-[4'-(*N,N*-dimethylamino)styryl]imidazo-[4,5-*b*]pyridine: effect of introducing a C=C double bond. *Photochem. Photobiol. Sci.* **2014**, *13*, 1476-1486.